Locomotion Experiments on a Planar Quadruped Robot with Articulated Spine

by

Karl Frederick Leeser

Submitted to the Department of Mechanical Engineering
in partial fulfillment of the requirements for the degree of

Master of Science in Mechanical Engineering

at the

MASSACHUSETTS INSTITUTE OF TECHNOLOGY

February 1996

Author .....
Department of Mechanical Engineering
January 19, 1996

Certified by ....
Marc Raibert
Professor of Electrical Engineering and Computer Science
Thesis Supervisor

Certified by ....
J. Kenneth Salisbury, Jr.
Principal Research Scientist, Mechanical Engineering
Thesis Reader

Accepted by .....
Ain Sonin
Chairman, Departmental Committee on Graduate Students

Locomotion Experiments on a Planar Quadruped Robot with Articulated Spine

by

Karl Frederick Leeser

Submitted to the Department of Mechanical Engineering
on January 19, 1996, in partial fulfillment of
requirements for the degree of
Master of Science in Mechanical Engineering

Abstract

Several quadruped robots have been built that are able to locomote, some by walking, some by trotting and running [22] [17] [11] [24]. A characteristic of these machines is a stiff back connecting the fore and rear legs. However, a look at running animals, and especially predators reveals a supple spine in place of the stiff back. This thesis explores the role of the spine in fast running via simulation of and experiments with a planar quadruped robot with an articulated spine. Experiments with the robot reveal that thrusting with the back can be used to augment the thrust provided by the legs. Simulation experiments suggest that motion of the back can be used to modify the impedance characteristic of the legs.

Thesis Supervisor: Marc Raibert
Title: Professor of Electrical Engineering and Computer Science

Thesis Reader: J. Kenneth Salisbury, Jr.
Title: Principal Research Scientist, Mechanical Engineering

Acknowledgments

Numerous people contributed to the success of this project. Some of them made it possible to bring the Planar Quadruped to fruition and to keep it in running order. Ben Brown, Kevin Brennan, and Peter Morley are such individuals. Then there are those who acted as a liason between my intentions and the beaurocracy of M.I.T. I would like to thank Marie Lamb and Lisa Inglese for providing that service. I am most grateful.

Foremost, there is the support group who guided me in my research and provided a healthy learning environment in which to work. I am always impressed by the quality level of engineers I have the opportunity to work with. Clearly, the Leg Laboratory at M.I.T. has been an environment that has fostered academic and intellectual growth within me as well as my work. To Dave Bailey, Peter Dilworth, Rob Playter, Jerry Pratt, and Robert Ringrose, thank you for your friendship and support. This core group will be sadly missed. To my advisor, Marc Raibert, thank you for your well managed guidance. You gave me the freedom to run with my project, but cautiously kept me on track. May I forever aspire to have a career as colorful as yours.

Finally, there is the one shining light in the whole process who kept me sane. To the love of my life, my gemini twin, I am forever indebted to you for putting up with 1000 miles between us while I completed my graduate career. I am forever in your debt. This work is dedicated to you, Becky Lau.

Karl Leeser
January 19, 1996

Contents

List of Figures

List of Tables

Chapter 1

Introduction

While humans walk and run bipedally, animal species that are primarily bipedal are few in number. Of these, humans, ostriches, and kangaroos are the most notable. The remaining legged vertebrates are all quadrupedal.

Mammalian quadrupeds have demonstrated some of the more amazing feats of the animal world. Horses are known for superb endurance. The fastest land animal is the cheetah, closely followed by several species of gazelle. Feats such as these invoke notions of great metabolic power and energetics. Is there something in their physiology that is common and responsible for their superior performance? A look at running ungulates and especially predators reveals an interesting structure connecting their fore and rear legs—a supple spine. Figure 1-1 demonstrates this remarkable organ in action.

This thesis explores the role of the spine in running via simulation of and laboratory experiments with a planar quadruped robot I built that has an articulated spine. The hydraulic machine has two telescoping, springy legs with actuated hips. Spanning the hips is an articulated spine composed of three segments with actuated joints.

The mechanical design of the Planar Quadruped is a simplification of the arrangement of an animal quadruped. I attempted to isolate the fundamental behavior of the spine and capture it using the simplest mechanical arrangement possible. Although viewing films of cheetahs in pursuit of prey will attest to their remarkable ability to quickly change direction of travel with severe twisting motions of the spine, the most basic behavior of the spine during quadruped running is bending [14]. In contrast, Japanese researchers built a robot with a spine that primarily twists in order to study recovery to land on one's feet during a fall [30].

The Planar Quadruped only has two legs, one fore and one aft. This arrangement treats the front and rear *pairs* of legs each as a single unit. This simplification has basis in fact. Domestic cats frequently run with a half bound, where the rear feet contact the ground nearly simultaneously [14]. Such a motion is akin to replacing the pair of rear legs with a single leg.

Experiments with the Planar Quadruped robot reveal that thrusting with the back can be used to augment the thrust provided by the legs. I performed an experiment that exploits the series kinematic connection between the back and the foot. In the experiment, motion of the back was used to modulate the energy state of the leg spring.

Simulation experiments suggest that motion of the back can be used to modify the impedance characteristic of the legs. I performed two experiments to explore this possibility. The first commanded the joints of the back to open loop static positions during various parts of the locomotion cycle to reduce the rate of compression of the leg springs. The second attempted to servo these joints off of the ground vertical reaction force to simulate a virtual vertical spring. Although only partially successful, the second appears very promising. In the process, I developed two interesting gait controllers that coordinates the behavior of the robot to produce a bounding gait with significantly larger leg workspaces than a previous Leg Lab quadruped robot [11] [24].

Chapter 2 looks at uses of the trunk and spine for animals that have been identified in the literature. Chapter 3 describes the hardware used in experiments, presents a review of the running

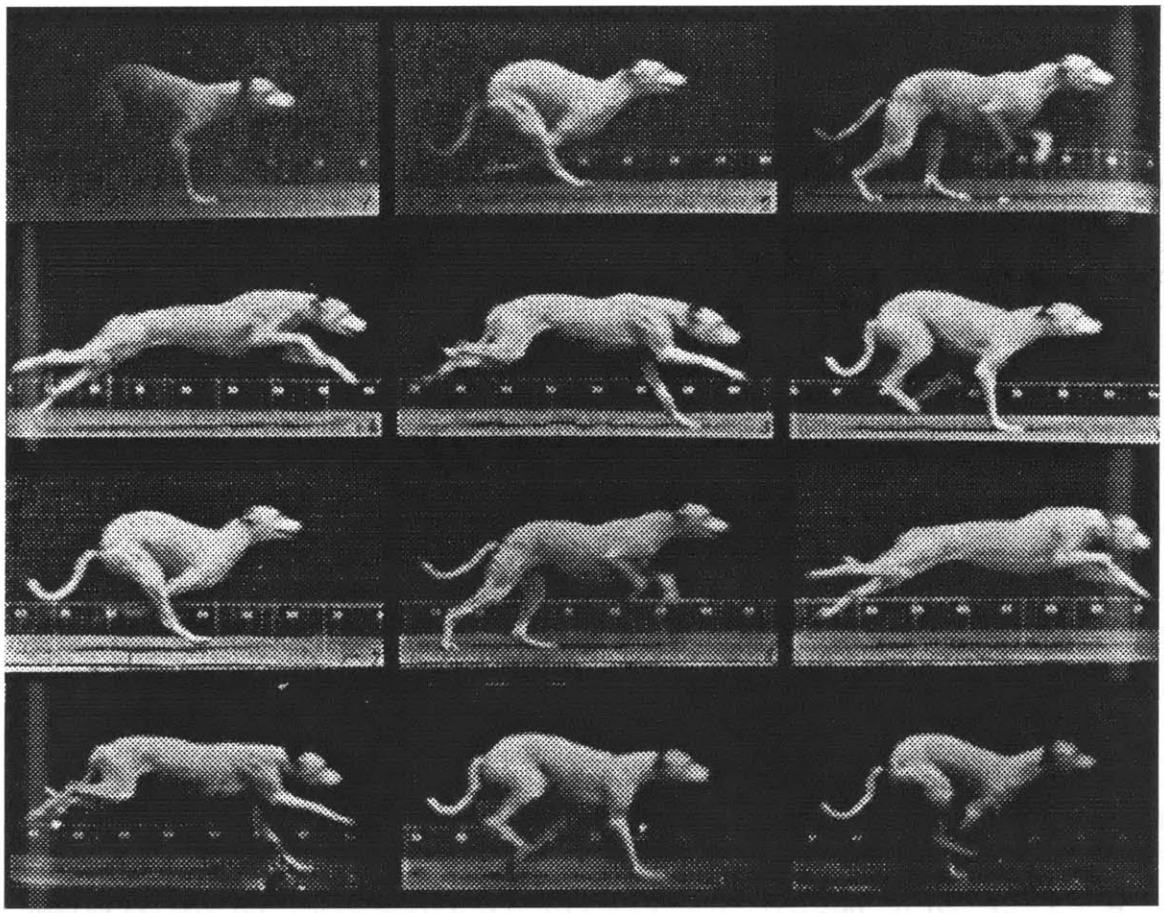

Figure 1-1: Successive frames of a galloping dog. The sequence begins with the photo in the upper left and proceeds left to right, top to bottom. Maximum spinal flexion occurs during the crossed flight phase shown in frames 2, 7, and 12. Maximum extension is shown in frames 4 and 9. Photograph from [23], Plate 710. Reprinted with permission from Dover Publications, Inc.

algorithms that provide a basis for control of the robot, and describes the bounding gait controller used in experiments. Chapter 4 proceeds to discuss potential roles for the back in robot locomotion. Chapter 5 presents experiments, consisting of thrust augmentation, half bound control, and impedance servoing. Finally, Chapter 6 concludes the thesis with recommendations for future work.

Chapter 2

Uses for the Spine and Trunk

In nature, quadruped mammals have adapted to a variety of modes of running and the function of the spine has become correspondingly specialized. For instance, in metalocomotory running animals, the spine's primary function is shock absorption. In carnivores and rabbits, the spine is suited to acceleration and speed respectively [12]. Despite these specializations, a review of the literature on the biomechanics of cursorial quadrupeds reveals several commonly accepted general roles for the spine and trunk. These roles are to increase leg length, to provide auxilliary power to the legs, and to store and transfer energy.

2.1 Kinematic Advantages

Classical biomechanical texts indicate that the kinematic advantage of increased leg mobility is the primary benefit cursorial quadrupeds receive from a supple spine. Portions of the spine function as a kinematic extension of the leg. This physiological adaptation effectively increases leg length. Gray discussed how increased effective leg length due to spinal extension in cheetahs and ungulates increased the stride length [13]. Increased stride length is generally considered to increase speed.

Kinematically, the segments that make up the spine and legs are serially connected. In this series mechanical connection, motions at the foot result from the sum of the motions of all the joints in the chain, from the spine through the leg. By serially imparting motion on the feet by both back and leg muscles, a higher leg *velocity* results, increasing the sweep speed [14]. Thus, the spinal extension speed contributes to the overall speed of the animal [15]. This arrangement is significant because muscles are inherently velocity-limited actuators. That is, there exists a maximum muscle velocity beyond which no force can be exerted [16].

2.2 Auxilliary Power

Classical texts also acknowledge a muscular advantage. Gray suggested that the musculature of the back provides substantial mechanical power during spinal contraction that augments the power provided by the legs [13]. Alexander noted that at high speeds, the large power requirements of moving the legs cannot be satisfied by the leg muscles alone. Back muscles must be responsible for the additional required muscle power [1]. Additionally, flexion of the spine during rear leg stance serves to further accelerate the forelegs, more than is possible using the muscles of the rear legs alone [14].

2.3 Energy Storage and Transfer

Recently, the spine has been suggested as an important energy store in galloping quadrupeds. Muscles, ligaments, and tendons in legs have long been identified as spring-like mechanisms that store elastic energy and serve to decrease the metabolic cost of running [2] [4]. McMahon proposed

that a running animal can be modelled as a collection of vertical mass-spring oscillators [21]. Raibert and his coworkers built running robots based on this paradigm [26] [25].

The recent attention given to the energy storage role of the spine may be attributed to much former biomechanical analysis that only considered work done on an animal's center of mass. In departure from this philosophy, most notably, Alexander has considered the internal energy associated with the various parts of running quadrupeds. Alexander argued that if the fore or rear legs of a running quadruped were considered isolated conservative systems, then the internal kinetic energy associated with swinging the legs forward and backward should be approximately equal. However, in animal experiments, Fedak et al. found that the internal kinetic energy of the forward swing is markedly less than that for the backward swing [10] [5]. Alexander surmised that some form of energy transfer between legs must occur to accomodate the fluctuation in energy [2] [4] [3].

Specifically, Alexander surmised that the fluctuating kinetic energy due to the swinging of a quadruped leg could be temporarily stored elastically in the back and later retrieved by another leg. The most likely candidate structure for elastic storage is the aponeurosis of the longissimus thoracis et lumborum muscle [5] [3]. The longissimus muscle is the dominant elastic structure in the back [6].

Other elastic structures in the trunk have been suggested. Alexander noted that the aponeurosis, strained during spinal flexion, must have counterparts during spinal extension. He identified the facia lata (between femur and pelvis) as such an elastic mechanism, but conceded that it acting alone could not transfer energy to the fore legs [4]. Similarly, Alexander noted that the muscles and tendons used to rotate the shoulders and hips might serve a secondary purpose, in addition to actuation, of auxilliary elastic energy storage [5].

Alternatively, quadrupeds may be able to store kinetic energy in the trunk. McMahon used a simple spring-mass oscillator model of running to compare several quadruped gaits. In application of the model, McMahon assumed that elastic energy stored in a stance leg entering flight was transferred to other stance legs. In passing, he proposed that this transfer occurred by converting the elastic energy to an intermediate kinetic form and suggested that the rotational motions of the trunk accounted for such storage [21].

2.4 Application to Robot Quadrupeds

The roles identified herein for the spine and trunk are commonly associated with animal backs. Are these issues of any practical significance to the control of a quadrupedal robot? Chapter 4 will attempt to answer this question by developing control concepts that seek to capitalize on the benefits outlined herein. Later, experiments with and simulation of a planar quadruped robot will be used to verify some of those strategies.

Chapter 3

Experimental Robot

In order to study the role of an articulated spine in quadrupedal locomotion, I built the machine diagrammed in Figure 3-1. As shown in Figure 3-2, experimental hardware consisted of the quadruped robot, a planarizing boom, a treadmill, and control computers.

3.1 Robot

I built the planar machine in Figure 3-1 to study the role of an articulated spine in quadrupedal running. The hydraulic machine has two telescoping legs with actuated hips, one fore and one aft. Although the Planar Quadruped only has two legs, the arrangement simplifies the design yet captures the dominant leg behavior found in bounding. Spanning the hips is an articulated spine composed of three segments with actuated joints. The center section houses I/O and servo electronics and hydraulic power distribution. The outboard vertebra support actuation for the hip and spinal joints. A planarizing boom constrains the motion of the quadruped to a plane, allowing horizontal and vertical translation of the robot and rotation about the pitch axis. Computers on and offboard control behavior. The robot stands approximately .84 m high with the legs at the nominal length. With the back straight, the hip to hip spacing is approximately .97 m. The Planar Quadruped weighs 25 kg. Figure 3-3 diagrams the robot's kinematic arrangement. Figure A-1 in Appendix A shows the kinematic notation used to describe the Planar Quadruped.

The aim of the Planar Quadruped robot is to represent the minimum hardware necessary to begin studying limber-backed quadruped running. The articulated spine I built has three segments, the minimum necessary to exhibit both standing and travelling wave behavior. The relative scaling of the leg lengths versus hip-to-hip spacing has been patterned after the domestic cat as found in [8]. The kinematics of the Planar Quadruped design allows a large workspace in a slim, antisymmetric package. The extent of the workspace reaches from the extended pose of first flight to the crossed pose of second flight as shown in Figures 3-5 and 3-4.

The Planar Quadruped contains two telescoping legs that terminate in revolute hips. The structure of the leg has been constructed from a custom extrusion that doubles as the actuator body. The low-friction hydraulic leg actuator contains a single ended piston with the maximum area present during extension when maximum force is required. Like other Leg Lab robots, in series with the actuator piston is an air spring. A pneumatic line supplies pressure to the air spring, regulated to between 10 and 15 psig. The lower end of the leg is connected to a passive foot soled with rubber foot pads. The foot contains an electrical foot switch used to detect contact with the ground.

Connecting the hips is the three-link, articulated spine. The center section is constructed of a welded tubular aluminum cage. The cage protects two I/O-CPU board electronics packs piggybacked atop each other. Hydraulic power distribution occurs beneath the cage via a manifold. The planarizing boom attaches to the rear of the cage.

The outboard sections of the spine (vertebra) have a carbon fiber and aluminum load-bearing structure supporting the hip and spinal actuators in a cantilevered, over-under arrangement. The

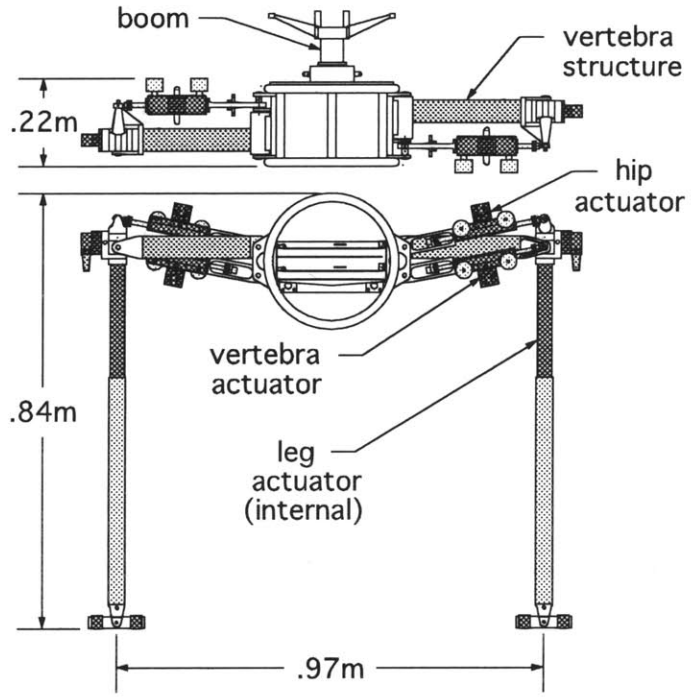

Figure 3-1: Planar quadruped robot. The machine contains an articulated spine composed of three segments. The center section houses I/O and servo electronics and hydraulic power distribution. The outboard vertebra support actuation for the hip and spinal joints. The legs telescope and are shown in the extended position. Hydraulic hoses and wires are not shown for clarity.

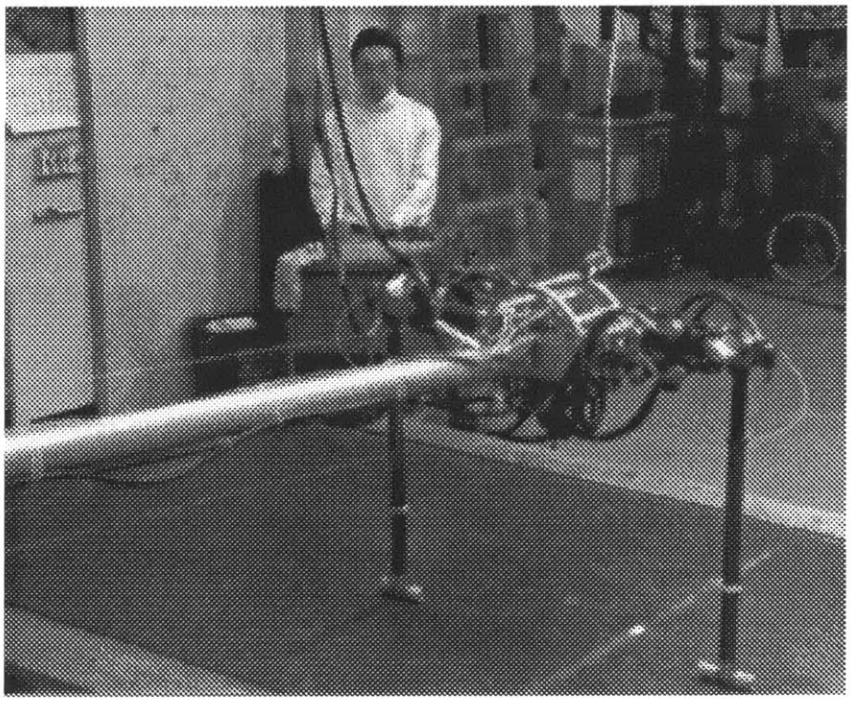

Figure 3-2: Test setup. Experimental hardware consisted of the quadruped robot, a planarizing boom, a treadmill, and control computers. In the background, the author mans the joystick for supervisory control of the robot's velocity.

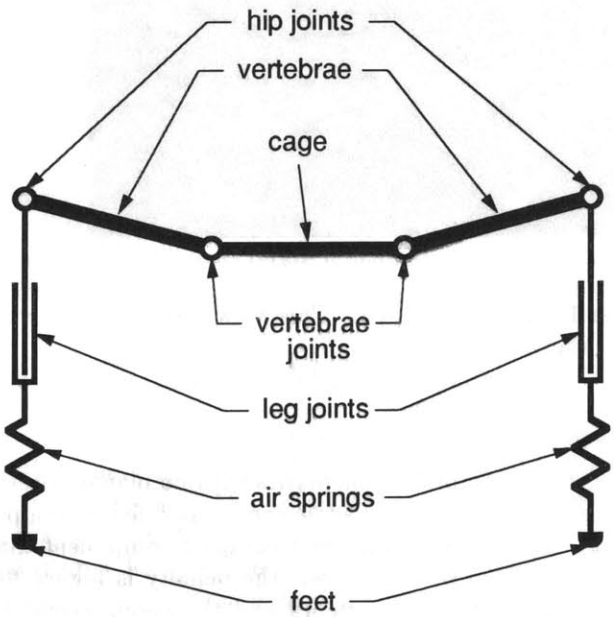

Figure 3-3: Kinematic configuration. Circles represent revolute joints. Each of the legs contains a single actuated prismatic joint in series with a pneumatic airspring. The darkened links indicate the segments comprising the spine: two outboard vertebrae and a connecting cage link.

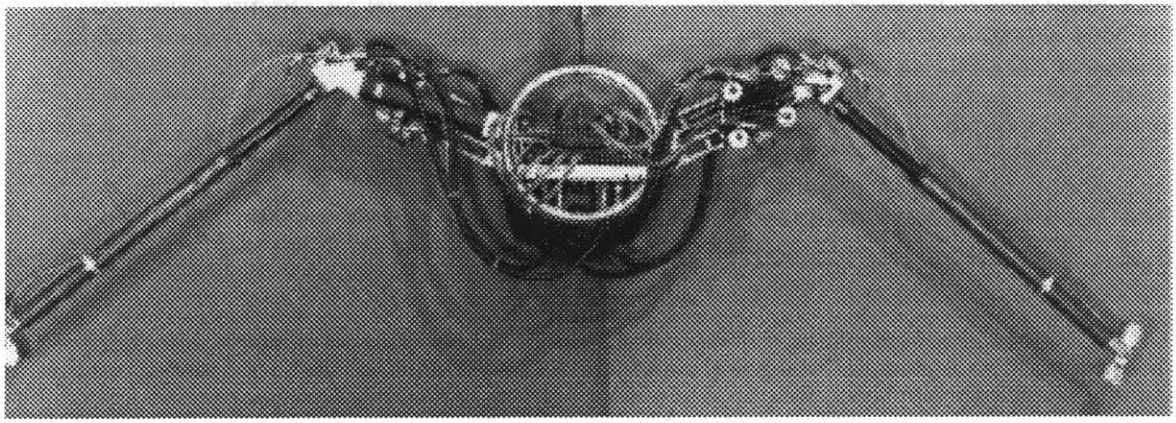

Figure 3-4: Workspace of the Planar Quadruped. This view is at maximum spread. (≈6% full scale).

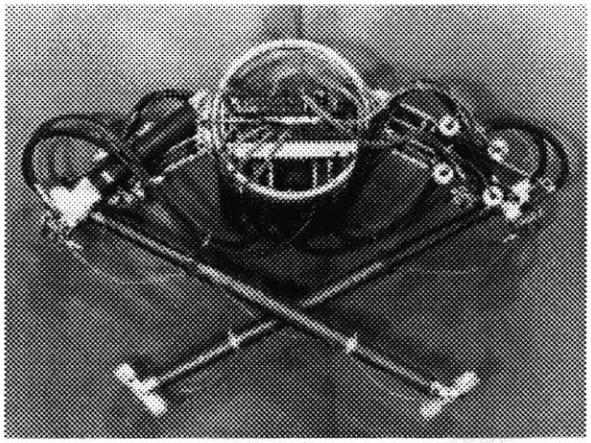

Figure 3-5: Workspace of the Planar Quadruped. This view indicates the crossed-legged pose characteristic of second flight. (≈6% full scale).

over-under actuation design results in simplified kinematics with no planar offsets; the same kinematic transformation between actuator length and angle can be used for both hip and spinal angle calculation (See Appendix A.2). This design results in a compact component that is lighter than a corresponding uncantilevered arrangement. However, the penalty is higher bearing loads due to off-axis loading. With the actuators on the vertebra and the boom weight loading the cage, weight is evenly distributed across the spine. Placement of the actuators on the vertebra increases the system's pitch inertia, decreasing the bounce frequency of the system, and reducing actuator control effort requirements.

A 20 MPa offboard hydraulic pump supplies mechanical power. Highly flexible rubber hoses distribute power. The hoses are routed along joint axes to minimize external torques about joints. Low friction actuation is accomplished by eliminating moving seals in the hydraulic actuators and allowing a small amount of leakage around the piston. Moog aircraft servovalves with 90 Hz bandwidths modulate flow to the piston. The hydraulic design allows the hip and spinal actuators to have a 2600 N nominal maximum thrust. The actuators are instrumented with Data Instruments MLT linear pots to measure piston position. Data Instruments Model SA pressure transducers on the body actuators estimate the differential pressure across the piston, used for pressure damping in some of the servo laws.

3.2 Planarizing Boom

The planarizing boom, spanning 3.843 m from the wall to the robot, constrains the motion of the quadruped to a plane, allowing horizontal and vertical translation of the robot and rotation about the pitch axis. The boom also acts as an umbilical, supporting electrical communication, hydraulic supply and return lines, and an air hose. The boom structure is a 7.6 cm OD, 1.5 mm wall alluminum tube compressional member with gimballed ends. Steel cables maintain the robot parallel to the wall. An axle between the robot mount and the boom allows pitch rotation. Potentiometers in the gimbal at the wall end of the boom are used to estimate the translations of the robot in the horizontal running and vertical directions and a single potentiometer fastened to the pitch axle gives pitch information. The boom is slightly compliant with a fundamental frequency of approximately 9.2 Hz.

3.3 Treadmill

The treadmill is an endless belt with a maximum linear velocity of 5 m/s. The treadmill is hydraulically powered and has a rubber running surface approximately 1.5 by 5 m. A tachometer measures the velocity of the treadmill surface. The speed of the treadmill is controlled by the driver.

3.4 Control Computers

Computing power for the quadruped running experiments was provided by a five node Inmos transputer network. Two nodes, each coupled to an I/O board and located on board the robot, read sensors and run servo code at 500 Hz servo loops. One node, also coupled to an I/O board, reads joy stick and slider information and makes this information readable to the rest of the network. The final nodes run task level (state machine) control code and kinematic calculations at approximately 150 Hz. Connection to the Unix LAN occurs through the task level conrol nodes.

3.5 Review of Running Algorithms

Before proceeding to describe possible robot experiments utilizing an articulated spine, it is useful to review the algorithms developed in the Leg Lab to control balance and dynamic running in one-, two-, and four-legged robots. This tutorial will provide a framework for understanding the control approaches suggested in the next chapter.

The running algorithms developed in the Leg Lab are based on a three-part control scheme. This scheme decomposes control of running into the separate execution of three primary control actions: regulation of forward running speed, hopping height, and body attitude. These actions are summarized below. See [26] for more details.

3.5.1 Forward Running Speed

For a running biped robot, speed control occurs via placement of a foot relative to a *neutral point* prior to touchdown. The neutral point is defined as a point on the ground about which the center of mass of the robot traverses a symmetric trajectory during stance. Displacement of the foot from this neutral point skews the symmetry of the robot's center of mass trajectory resulting in a net acceleration or deceleration. The following law, incorporating a velocity stability term (the neutral point) and an error correction term, determines the desired swing leg foot position:

$$x_{d_f} = \frac{\dot{x} T_s}{2} - K_{\dot{x}}(\dot{x}_d - \dot{x}),$$

where

x_{d_f}	is the planar displacement of the foot from the projection of the center of mass,
T_s	is the duration of the most recent stance period,
$\dot{x}$	is the average forward speed,
$\dot{x}_d$	is the desired forward speed, and
$K_{\dot{x}}$	is a speed gain.

The operator specifies the desired speed, $\dot{x}_d$, with a joystick. The controller measures the duration of the stance period and updates T_s every step. The speed signal in the above computation, $\dot{x}$, is the estimated speed of the center of mass.

3.5.2 Hopping Height

Hopping is a resonant oscillation of the body mass on springy legs in a gravitational field. This oscillation would normally decay, but thrust is provided once per cycle to force the oscillation.

For a given thrust and a constant horizontal velocity of the center of mass, the magnitude of the hopping oscillation converges to a steady state altitude.

The Leg Lab robot's legs have springs in series with a hydraulic actuator. Movement of the actuator changes the rest position of the spring. This action changes the energy state of the spring, introducing energy as necessary to compensate for system losses experienced over the previous bounce cycle. When the leg spring reaches maximum compression, the leg actuator is servoed to

$$l_d = l_{nom} + \Delta l_{thrust}$$

where

l_d	is the desired leg actuator length
l_{nom}	is the nominal length of the leg actuator prior to thrusting, and
Δl_{thrust}	is the desired thrust.

The amount of thrust, Δl_{thrust}, is typically kept constant.

3.5.3 Body Attitude

Maintenance of body attitude is crucial to good robot hopping performance. For hopping, regulation of body attitude occurs once per bounce cycle by application of a corrective torque between the leg and hip in response to an angular error about the pitch axis. This action normally happens during stance, while the foot has traction on the ground.

3.6 Stiff-Backed Bounding

All experiments performed within this work incorporate or begin with a bounding gait. I present the control of this gait below to facillitate understanding of what follows in discussions of experiments.

A bounding gait is a quadruped gait characterized by alternately hopping on the fore and rear legs. The center of mass bounces and usually[1] experiences a regular oscillation in pitch.

3.6.1 Gait Control

A cyclic state machine coordinates the behavior of the Planar Quadruped. Similar to the three-part controller used for hopping in previous Leg Lab robots, it specifies when each of the three primary control actions are applied during the locomotion cycle. These control actions are regulation of forward running speed, hopping height, and body attitude. However, some of the control actions used for a bounding robot differ slightly from the actions described for biped robots. The following section points out these differences and describes some of the details of implementation. Table 3.1 outlines the state transition sequence used in stiff-backed bounding.

Forward Running Speed

A single bounding step is an asymmetric activity. However, over pairs of consecutive steps (a single stride), the behavior of a bounding robot is symmetric. This fact coupled with a favorable mass distribution allowed placement of the foot relative to the hip to be used to control forward running speed. The following law determines the desired foot position:

$$x_{d_f} = \frac{\dot{x}_f T_s}{2} - K_{\dot{x}}(\dot{x}_d - \dot{x}_f),$$

[1] Coordination of hip torques and leg forces can result in a gait whose pitch doesn't oscillate, but is technically a bound.

State	Trigger Event	Actions
LOADING$_A$	Leg A touches down	Zero hip torques on leg A Maintain leg A long length Servo vertebra A straight Position leg B for touchdown Maintain leg B length Servo vertebra B straight
COMPRESSION$_A$	Airspring A reaches positive support	Zero hip torques on leg A Maintain leg A long length Servo vertebra A straight Position leg B for touchdown Maintain leg B long length Servo vertebra B straight
THRUST$_A$	Airspring A reaches maximim compression	Zero hip torques on leg A Thrust with leg A Servo vertebra A straight Position leg B for touchdown Maintain leg B long length Servo vertebra B straight
UNLOADING$_A$	Airspring A reaches negative support	Zero hip torques on leg A Shorten leg A Servo vertebra A straight Position leg B for touchdown Maintain leg B long length Servo vertebra B straight
FLIGHT$_A$	Leg A leaves ground	Position leg A for touchdown Lengthen leg A Servo vertebra A straight Position leg B for touchdown Maintain leg B length Servo vertebra B straight

Table 3.1: Finite state machine for stiff-backing bounding. The state shown in the left column is entered when the event listed in the middle column occurs. The states advance in the listed order continuing on to similar states for the other leg, beginning with COMPRESSION$_B$ and ending with FLIGHT$_B$. All lengths above refer to leg actuator lengths.

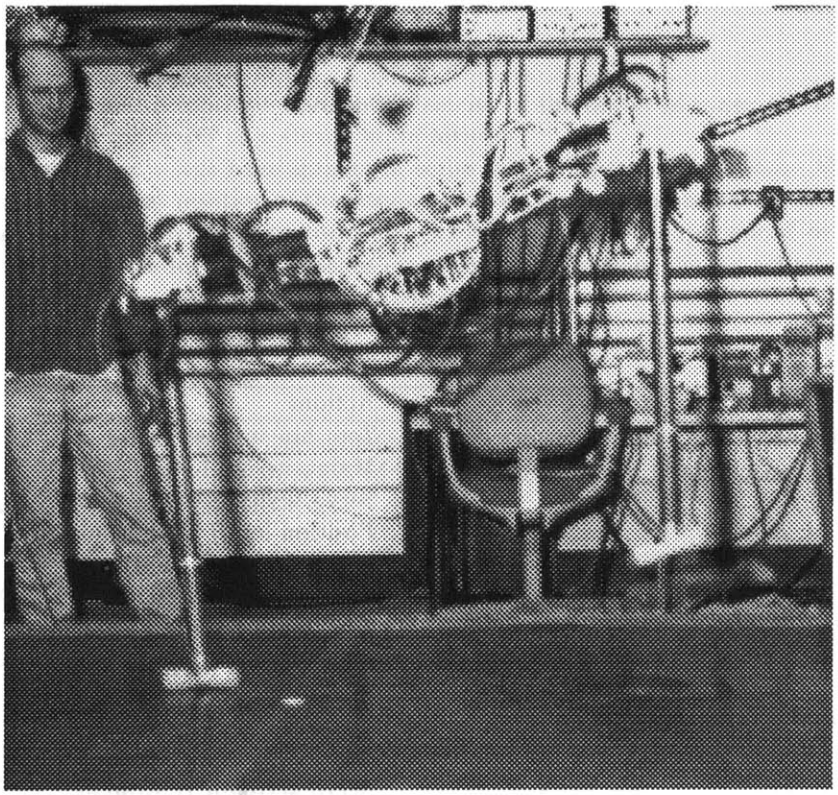

Figure 3-6: Robot in action. Here, the Planar Quadruped runs on the treadmill with a bounding gait.

where

x_{d_f}	is the planar displacement of the foot from the projection of the hip,
T_s	is the duration of the most recent stance period,
$\dot{x}_f$	is the average forward speed,
$\dot{x}_d$	is the desired forward speed, and
$K_{\dot{x}}$	is a speed gain.

The operator specifies the desired speed, $\dot{x_d}$, with a joystick. The controller measures the duration of the stance period and updates T_s every step. The speed signal in the above computation, $\dot{x}_f$, is nominally the speed of the center of mass. However, on the Planar Quadruped, it is the speed of the point where the boom attaches to the robot that is measured. The controller computes this speed as a sum of the inertial robot speed and the inertial treadmill speed:

$$\dot{x} = l_b \sin(\dot{\theta}_b) + \dot{x}_t$$

where $\dot{x}$ is the velocity estimate, l_b is the length of the boom, $\dot{\theta}_b$ is the approximated angular velocity of the boom in the horizontal direction, and $\dot{x}_t$ is the measured treadmill velocity. The controller estimates the speed of the center of mass, $\dot{x}_f$, by filtering $\dot{x}$ at the bounce frequency, or approximately 2 rad/sec, and passing the signal through a zeroth order hold when the robot enters the FLIGHT states.

Body Attitude

Attitude stability occurs passively for bounding. That is, the Planar Quadruped does not actively correct body attitude. During stance, the hips simply servo a zero torque. This passive result reported previously in [28] occurs due to the symmetric nature of bounding when considered over a complete stride.

3.6.2 Servos

The gait control actions of regulation of forward running speed, hopping height, and body attitude result in position and torque servo level commands. Position and torque control servos administered these commands.

Position Control

Foot placement calculates a static desired foot position in inertial space. However, the high pitch velocity of the Planar Quadruped creates a tracking problem in hip actuator space. A typical trajectory involves a fast transient and just prior to touchdown, a steady state ramp. The compensator takes the form of a PID controller with flow feedforward:

$$u = K_p(e_w) + K_d(\dot{e_w}) + K_i(\int e_w \ dt) + K_Q(\dot{w}_d),$$

where

e_w	is the actuator position error, $w_d - w$
w_d	is the desired actuator position,
w	is the actuator position,
$\dot{w}_d$	is the desired actuator velocity, and
K_i	are gains.

In practice, the filter is really a lead-lag filter due to the approximate nature of the discrete differentiation method employed. As implemented, the third term incorporates a resetting integrator that resets at zero crossings, improving the transient response. Although, the static positioning accuracy of the flow control servovalves is very good due to the inherent integrator present in the servovalve, the integrator in the compensator was added to improve steady state tracking. Appendix B describes the filters used.

The leg and vertebra actuators were adequately compensated using proportional controllers with rate feedback:

$$u = K_p(w_d - w) - K_v(\dot{w}),$$

where

w_d	is the desired actuator position,
w	is the actuator position,
$\dot{w}$	is the actuator velocity, and
K_i	are gains.

Torque Control

Pressure information from the vertebra and hip actuators facilitated torque control. The torque servo is a pressure controller with positive velocity feedback to approximately invert the dynamics of viscous friction in the hydraulic actuators:

$$u = K_P(P_d - P) + K_f(\dot{w}),$$

where

P_d	is the desired actuator pressure, $-\frac{\tau_d}{Ar}$ for the hips and $+\frac{\tau_d}{Ar}$ for the vertebra,
P	is the actuator pressure,
τ_d	is the desired torque,
A	is the actuator cylinder area,
r	is the instantaneous actuator moment arm about the joint,
$\dot{w}$	is the actuator velocity, and
K_i	are gains.

3.6.3 Initiation of Bounding

Bounding experiments began with the robot standing on the treadmill with both feet on the ground. The operator signalled bounding to begin by invoking the following automated launch strategy:

- Begin with the *pronk* gait controller
- Thrust as much as possible with both legs to launch
- Bounce once to compress the airsprings
- Differentially thrust as much as possible to impart a torque on the body and begin pitching motion
- Switch from *pronk* to *bound* gait controller and recover.

A *pronking* gait is one in which the robot moves by hopping on both legs simultaneously. Since both legs are used together, the Planar Quadruped's pronking gait used the *virtual leg* abstraction utilized previously for trotting and pacing in Raibert's quadruped[28]. This construct consisted of several rules for governing the behavior of the individual legs to emulate a single virtual leg. In particular, both legs must

- Touch down and take off simultaneously
- Reach a position relative to the hips for foot placement equal to the distance specified for the virtual leg with respect to the center of mass
- Apply equal forces and torques during stance, equal to half of the forces and torques specified for the virtual leg.

Pronking began by thrusting as much as possible with both legs. While ballistic, the pronk controller servoed the leg actuator lengths to produce the commanded virtual leg length. For the launch procedure, the specified foot position was zero ($x_{d_f} = 0$).

During stance, the pronk controller equalizes leg forces by servoing the airspring length. Since the force-deflection curve of the airspring is monotonic, the length of the airspring is a measure of the leg force. Thus, equalizing the airspring length equalizes the leg forces. The controller specifies a desired actuator length according to

$$\begin{bmatrix} w_{d_1} \\ w_{d_2} \end{bmatrix} = \begin{bmatrix} w_1 \\ w_2 \end{bmatrix} + \begin{bmatrix} \frac{1}{2} & -\frac{1}{2} \\ -\frac{1}{2} & \frac{1}{2} \end{bmatrix} \begin{bmatrix} l_1 \\ l_2 \end{bmatrix},$$

where

w_d	is the desired actuator length,
w	is the actuator length,
l	is the airspring length, and
$_i$	the subscript denotes the leg number.

Imparting a large torque to the robot begins the pitching motion characteristic of the bound. Differentially thrusting the legs provides both a force to and a moment about the center of mass according to

$$\begin{bmatrix} F_b \\ \tau_b \end{bmatrix} = \begin{bmatrix} -1 & -1 \\ -r & r \end{bmatrix} \begin{bmatrix} f_1 \\ f_2 \end{bmatrix}$$

where

f	is the leg force applied to the ground,
r	moment arm of the leg about the center of mass,
F_b	is the resultant force on the body,
τ_b	is the resultant torque on the body, and
i	the subscript denotes the leg number.

When both feet left the ground, the pronk gait controller switched to the bound gait controller which assumed control once leg 1 contacted the ground. Recovery occurred using the bound gait controller. No special recovery procedure was necessary or used.

I was not able to initiate bounding from a standing start and thrusting differentially. Additionally, torquing the hips produced undesireable horizontal acceleration of the body. However, with both airsprings compressed by the momentum of the body, after the first bounce, additional energy is available to torque the body and differential thrusting proved adequate.

Chapter 4

Articulated Spines and Robot Locomotion

In Chapter 2, three roles for a spine in animals were identified. The were kinematic extension of the legs, augmentation of leg actuator effort, and energy storage and transfer. In the previous chapter, the approach used in previous Leg Lab robots was summarized to provide a framework for understanding the control approaches discussed in this chapter. In this chapter, I consider experiments to study possible roles for an articulated spine in legged robot locomotion.

The many possible uses for a robot spine do not need to be addressed in a single experiment. Justification comes from Mother Nature; she has engineered her creatures to specialize spinal function. For example, the cheetah isn't a model of efficiency. Rather, it's design is about optimal for maximum speed, appropriate for a predator [14].

4.1 Virtual Biped

Biomechanical texts claim that the primary role of the spine is to provide a kinematic extension of the legs. In the limit, an initial experiment could consider each vertebra and its nearest telescoping leg as comprising a single articulated leg. Since the workspace of this configuration allows the foot to pass under the center of mass, in theory, a coordination scheme could be determined to emulate an artificial spring along the *virtual* leg connecting the center of mass and the foot. This coordination scheme would also apply torques to the body to correct posture. Thus, control of the Planar Quadruped would simplify to control of a virtual biped. A diagram of this control scheme is shown in Figure 4-1.

Such an experiment would allow the control of some back motion to transparently fit into the existing control framework developed for earlier robots. Controllers for two-legged hopping machines are well developed [26]. In fact, the controllers for the Leg Lab bipedal and quadrupedal robots are simply generalizations of a one-legged hopping controller [24].

Such an experiment leads to pitfalls, however. The real workspace of each of the virtual legs is highly asymmetric with respect to the center of mass. This means that the robot could only operate at low velocities before the virtual leg would be unable to reach a desired foot position in one leg for foot placement, or sweep to a symmetric take off position in the other. In addition, a coordination scheme that emulates a virtual leg spring must dissipate lots of power in simulating the passive component. That defeats the purpose of the mechanical leg spring. Finally, an approach that seeks to control a machine with an articulated back by treating it as a biped has simply redefined the problem to control of a machine with articulated legs.

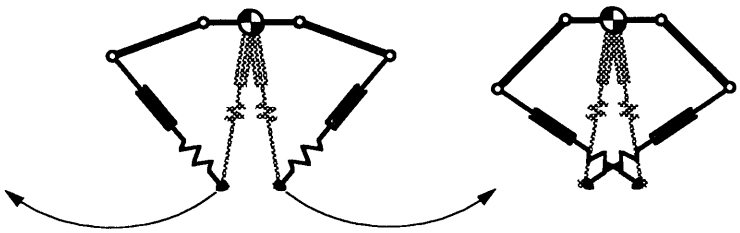

Figure 4-1: Virtual biped control construct. Each vertebra and its nearest telescoping leg comprise a single articulated leg. Along the *virtual* leg connecting the center of mass and the foot lies an artificial spring. This construct could simplify control of the Planar Quadruped to control of a virtual biped. The diagram on the left shows the virtual feet .35 m apart although the workspace allows the separation to be much greater. The diagram on the right shows the virtual feet at a workspace boundary, with the legs crossed, but .35 m apart. Thus the region of possible symmetric virtual bipedal motion is only $\pm .35$ m.

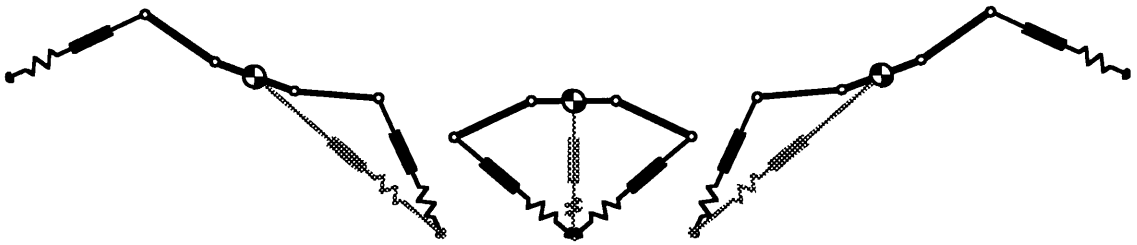

Figure 4-2: Virtual monopod control construct. The two legs of the Planar Quadruped are sequentially coordinated over a stride to emulate one springy leg. Such a strategy would require landing on the fore leg, transfering support below the center of mass, then taking off from rear leg. Unlike the virtual biped control construct, the full workspace of both legs can be used and monopod-like symmetry is preserved.

4.2 Virtual Monopod

Consider then a virtual monopod, where both legs are used to emulate a single leg. Unlike the virtual leg construct utilized previously for trotting and pacing in Raibert's quadruped[28] where two legs simultaneously emulate a single virtual leg, the approach suggested here is that the two legs of the Planar Quadruped are sequentially coordinated over a stride to emulate one leg. As depicted in Figure 4-2, such a strategy would require landing on the fore leg, transfering support below the center of mass, then taking off from rear leg. By transferring support under the body, the full workspace of both legs can be used and monopod-like symmetry is preserved. Thus, control would simplify to control of a virtual monopod.

Such a model is conceptually similar to McMahon's spring-mass model used for gait comparison as applied to a transverse gallop [21]. In this "kinematic wheel" concept, multiple legs contribute to a single, common resonant rebound of the body mass.

Domestic cats frequently run with a half bound where the rear feet contact the ground nearly simultaneously [14]. In such a gait, the second flight phase is either insignificant or nonexistent. The animal lands on its fore legs, loading them, and decelerates in both the horizontal and vertical

directions. The rear legs are extended foreward and support is essentially instantaneously transfered to the rear legs under the body. The legs are loaded and the body accelerates away both horizontally and vertically.

By utilizing the workspaces of both legs, a larger stride length results. Increased stride length due to increased flexion of the spine has the added benefit of increased duration of the support phases [14]. A longer support phase provides more time to exert control actions during stance, decreasing the necessary control bandwith while maintaining a high body velocity. A longer support phases also allows more time to impart energy onto the body. Therefore, power can be traded for time and lower power actuators can be used. The pursuit of a longer stride length is in departure to previous leg lab robot control where for fast running, stance time was minimized [19].

A larger leg workspace has other advantages. At high speeds, significant disturbances to body posture occur due to the impulsive acceleration of the leg when it strikes the ground. Disturbances can be minimized by accelerating the leg back in anticipation of touchdown and matching the ground speed with the inertial speed of the foot [19].

The difficulty in successfully implementing the virtual monopod approach on the Planar Quadruped robot appears to be a need for better positive/negative work control. In order to produce a single rebound using two legs, the foreleg needs to mostly absorb energy while possibly performing some negative work. The rear leg might undergo some positive work, but most of it would be negative. This leg behavior is in contrast to the natural impedance behavior of the leg; as a spring, it wants to perform equal positive and negative work. However, the legs of biological quadrupeds may not be totally conservative processes. In studies of a Nubian goat, researchers claim that the forelegs function as damping (control) elements. If a mechanism can be identified to override the natural springlike characteristic of the leg to produce this behavior, the result might be interesting.

4.3 Inertia Control

The requirement of instantaneous transfer of support specified above in the description of the virtual monopod can be relaxed to incorporate a second, albeit brief, ballistic phase. This second flight phase, or period of "crossed" or "second" flight as described in the biomechanical literature, occurs between the fore and rear leg stance phases. Bounding in such a manner would require the legs to pass briefly under the robot's center of mass. This trait has been shown to improve postural control of one and two-legged robots [27].

At very high velocities, bounding with a second flight phase may begin to resemble the manner which a dog or cat gallops. The body configuration as the machine leaves stance on its fore leg becomes increasingly tucked as velocity increases. This configuration may result in a mass distribution that is increasingly desireable; at high body speeds, the actuators may not be able to move and place the rear foot sufficiently fast. The foot moves with respect to the center of mass by virtue of its relative velocity and the body's rotational velocity. A small body inertia at this time would probably result in a high rotational velocity, decreasing some of the speed requirements of the rear leg actuators.

More importantly, with an articulated back, the machine could control its mass distribution during flight for greater position and velocity resolution for foot placement. However, for such a control approach to function acceptably, a good model of the body would be required. Moreover, inertia control wouldn't be limited to the second flight phase. In the primary ballistic phase, inertia control could be used to maximize flight time in order to optimize the distance travelled during flight, maximizing stride length.

Finally, as the body inertia as seen by the fore leg becomes increasingly different than that seen by the rear leg, a dynamic asymmetry will be introduced. This phenomenon is interesting because in the quadruped with its stiff back, the body inertia as seen by both legs is the same and roughly a 180 degree gait phase relationship results. With the introduction of dynamic asymmetry, a gait more similar to a gallop than a bound could appear.

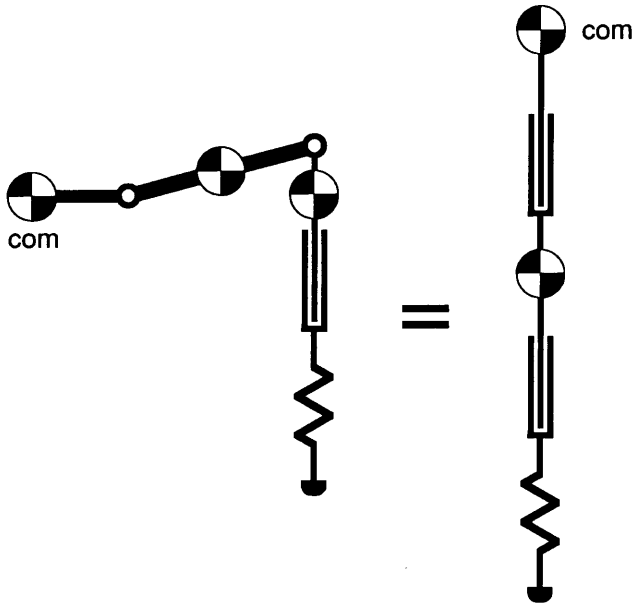

Figure 4-3: Series connection of certebra and leg joints. Motion of either actuator can produce motion at the base of the spring, altering its energy state. For that matter, the hip joint can be used to modulate leg spring energy as well, but in the robot bounding controller, the hip typically supplies zero torque during stance.

4.4 Modification of Leg Spring Impedance Characteristic

Alexander, Gray, and Hildebrand claimed that musculature in the backs of quadrupeds can somehow be used to fulfill the large power requirements of running. Koechling previously studied limitations on a robots performance while running at high speed [19]. These experiments found that one of the limiting factors to speed performance was the maximum velocity that the actuators could sweep the legs. An issue that wasn't directly addressed was the maximum leg thrust that the robot was capable of delivering to the leg spring.

As velocities increase, the dissipative nature of contact with and motion through the environment becomes increasingly pronounced. As such, the thrust delivered to the leg spring necessarily increases. However, at higher speeds the legs contact the ground with ever decreasing angles of incidence, approaching the friction cone. Without a coordination mechanism with the hips to reorient the reaction force vector more closely through the leg, the time available to supply thrust decreases even more. As the bounce frequency of the robot approaches the mechanical bandwidth of the actuators, use of a single, velocity-limited actuator to supply this thrust may be inadequate.

Since both the leg and vertebra joints are in series with the airspring, motion of either or both can react against the machine's center of mass and alter the energy state of the spring (See Figure 4-3). An interesting experiment would be to verify this principle and use back motion to supply thrust. Alternatively, the same principle can be used in a subtractive manner. Motion of the back can be used to modify the leg spring force-vertical deflection profile. Such an impedance control technique could be used to effectively soften the leg springs, allowing increased ground contact time as suggested in Section 4.2.

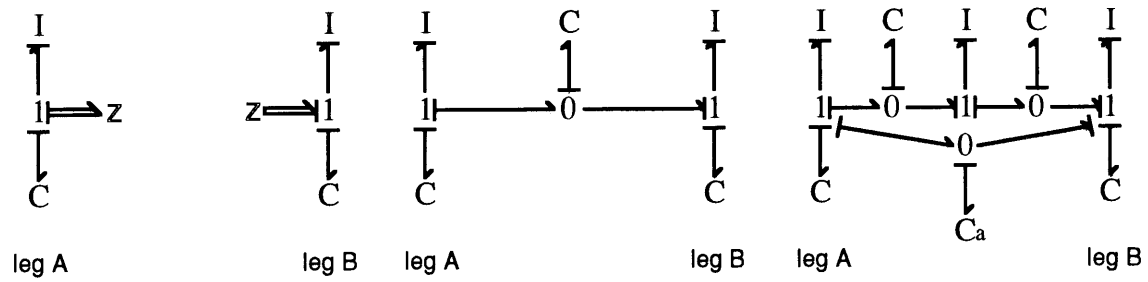

Figure 4-4: Simple model of quadruped using single degree of freedom oscillators to model the hoppers. A network spanning the oscillators obeys causality only if it appears as an impedance field to both hoppers as shown in the first column. The second column depicts the simplest conservative connection between the hoppers which is a spring-like element. However, as depicted in the third column, there are many combinations of generalized inertia and capacitor elements that satisfy the required causality. In the mechanical energy domain, inertia elements correspond to masses and rotational inertias. Capacitor elements correspond to compliances. Note the compliance labeled C_a. It satisfies causality and spans multiple joints much like the aponeurosis does. For the above figures, power flow is assumed positive from leg A to leg B.

4.5 Elastic Energy Storage

Approximately half of the metabolic energy required for running is saved due to elastic storage in the legs of men and kangaroos [7]. Similar energy savings has been suggested to occur in galloping due to elastic structures in the back [2]. An interesting robot experiment might be to attempt to duplicate some form of passive spring-like mechanism in the back and observe its effects on locomotion performance.

4.6 Energy Transfer

An energy transfer role for the spine is very compelling. Alexander suggested this role since the internal kinetic energy of quadruped fore legs is larger when the legs sweep back than when they sweep forward [5] [3]. The same is true for the hind legs, but since they occur out of phase, the notion of transfered energy accounting for the difference is appealing. One then might consider the front and back legs of a quadruped as two independent hoppers. If the back is treated as a separate mechanism from the hoppers, it might be possible to develop a model for an energy shuttling mechanism for the back which would modulate energy out of one hopper and into another.

Alexander suggested a spring model for the back and causality analysis shows that this is valid. Alternatively, a power transfer mechanism in the back could consist of a network of springs and masses as long as the network appeared as a generalized impedance field to either of the hoppers. Figure 4-4 demonstrates this conclusion via use of bond graph notation.

Although causality analysis suggests the necessary dynamics, it doesn't address how those dynamics should behave. I claim that all it needs is a single natural frequency.

Animal quadrupeds display a trot-gallop transition speed. They can gallop faster, and somewhere in between has been shown a speed at which they normally gallop with the most efficiency [18]. Given animal mass parameters and leg lengths, one can determine a stride frequency. One could imagine an energy-shuttling back tuned for that frequency. To gallop at higher or lower speeds (frequencies), actuator input might modulate a parameter of the back dynamics, say the spring stiffness and provide a ΔK. Thus, the back would perform most of the work passively and control input might only alter the natural frequency to match the stride frequency.

More interesting dynamics for the back might produce an energy transfer rate function that

was dispersive, that is, dependent on frequency. An example of such a function is that for the dynamics of a continuous beam. A beam model has wave energy whose speed of propogation is dispersive. A pass at generating a controller might be to modulate one of the beam parameters to modulate the group velocity. An appropriate parameter might be the beam stiffness. A stiffness controller could close a loop around stiffness and possibly control energy transfer rate in an open loop fashion. The beam model is appealing because its first mode behavior resembles that observed in animal backs.

Chapter 5

Experiments

Chapter 4 presented a number of possible areas of experimentation to learn more about the role of an articulated spine in legged locomotion. In this chapter, I present the results of several experiments examining some of those issues using a robot and dynamic simulation.

5.1 Vertebral Thrusting Experiment

One of the simplest experiments to try using the Planar Quadruped was to examine the effect of thrusting with the vertebral segments in addition to the normally applied leg thrust. Using the modified bounding state machine in Table 5.1, the vertebra were commanded to up and down 'α thrust angles' during various parts of the locomotion cycle. During stance, a vertebra was servoed to the down α thrust angle, while in flight, the same vertebra was servoed to the up angle.

5.1.1 Results

Experiments with the Planar Quadruped robot reveal that thrusting with the back can be used to augment the thrust provided by the legs. The result is motion of the back effectively modulates the energy state of the leg spring.

Figure 5-1 displays data from a trial run in which the gait was switched from stiff-backed bounding to bounding with vertebral thrust at approximately $t = 13.3$ seconds. For this experiment, the leg thrust was kept constant even after the onset of vertebral thrust. The commanded upper and lower α thrust angles were .315 and -.45 radians respectively. Prior to the gait change, the machine's hopping height is approximately constant at approximately .8 meters. After the gait change and a brief transient, the hopping height of the machine increases substantially, up to approximately 9.4 meters. As the hopping height increases, so does the angular excursion of the body in pitch. While the body has a 2.5 radian pitch amplitude during stiff-backed bounding, the amplitude increases to approximately 4 radians with the addition of vertebral thrust. With increased motion at the vertebra joint in addition to body pitch, it becomes increasingly difficult for the hip to place the foot as accurately as with stiff-backed bounding and some drifting in velocity appears.

Figure 5-2 displays similar data, but the leg thrust is decreased to zero. Vertebral (α) thrusting begins at approximately $t = 12$ seconds. The commanded upper and lower thrust angles was .31 and -.442 radians respectively. Both hopping height and pitch amplitude increase accordingly. At about $t = 13$ seconds, leg thrust is slowly decreased until it reaches zero. Hopping height and pitch amplitude decrease below their former values, but the robot maintains the hopping cycle with thrust provided solely by the vertebra.

Figure 5-3 displays data from a trial run at higher speed, $\dot{x} \approx 7$ m/s. The gait was switched from stiff-backed bounding to bounding with vertebral (α) thrust at approximately $t = 15.0$ seconds. The commanded upper and lower thrust angles was .089 and -.128 radians respectively. After a brief transient, the pitch amplitude increases slightly and the hopping height increases from about

.86 m to over .9 m. At about $t = 17.2$ seconds, leg thrust is decreased and hopping height and pitch amplitude return to their former values.

Figures 5-1– 5-3 demonstrate that vertebral thrusting influences hopping height similar to thrusting with the leg actuator. This fact is shown in the limit in Figure 5-2, where leg thrust diminishes to zero and the bouncing oscillation is maintained.

Motion of the rest length of the airspring provides thrust during stiff-backed bounding. In doing so, the leg actuator need only move the mass of the cylinder. However, in vertebral thrusting, the vertebra actuator must move the inertia of the vertebra plus the reflected inertia of the upper leg in addition to the cylinder mass. As such, the time required to effect a given deflection of the leg spring is substantially greater with vertebral thrusting only versus leg thrusting only. Thus, it was necessary to begin vertebral thrusting during the COMPRESSION state and continue into the THRUST state.

5.2 Planar Quadruped Simulations

Simulation is convenient for repeatedly testing control strategies under conditions which are difficult to consistently duplicate with the real robot. I created a simulation of the Planar Quadruped robot to study use of the back at high speed. High speed was determined to be above the trot-gallop transition speed of 3.3 m/s predicted for a 25 kg animal [20].

A model of the Planar Quadruped was coded using the Creature Library, a tool for creating dynamic computer simulations [29]. The simulations consist of equations of motion, ground contact models, a numerical integrator, a 3D computer graphics program, and user interface. The Planar Quadruped simulation consists of a collection of rigid bodies with masses and moments of inertia, connected by joints. Foot contacts with the ground are modelled as a spring-damper system that opposes penetration into the ground and prevents sliding on the surface.

The Planar Quadruped simulation seeks to replicate the dynamics of the physical robot. Link lengths are identical to the robot and the masses are distributed in a manner such that they sum to the total mass of the robot and integrate over the volume of the robot to approximately the inertias of the robot's links. Although the robot's leg springs are nonlinear, Hookean leg spring stiffnesses were determined such that the bounce frequency of the simulation approximately matched that of the robot. Leg spring stiffnesses of $K_{leg} = 4000$ N/m were chosen. Note that this is in close agreement to the leg springs predicted for a 25 kg animal of 4000 to 5000 N/m [9].

5.3 Half Bound Experiment

Section 4.1 and 4.2 discussed possible strategies for running experiments that attempted to exploit the kinematic advantages of large leg workspace when a supple spine is involved. The first experiment aimed directly at addressing this kinematic issue was the half bound experiment.

A half bounding gait is a quadrupedal gait in which sequential support on the forelegs is followed by a brief hop onto the rear legs which contact the ground simultaneously and function as a single leg. A support period on the rear legs is ensued by a flight phase. In this gait, the legs typically sweep far under the body and almost meet at a point approximately under the center of mass. With springy legs that tend to minimize ground contact time, this is not a trivial endeavor, however. Thus, in order for the legs to sweep far under the body, the effective leg spring stiffness must be reduced. Farley et al. found that leg spring stiffnesses are approximately constant over a wide range of speeds [9]. I surmised that motions of the back could be used to decrease the rate that the leg springs would otherwise load, effectively decreasing the leg spring stiffnes and increasing ground contact time and the angle swept by the legs during stance. Such modification of the *apparent* leg spring stiffness is what I refer to as modification of the leg spring impedance characteristic.

Table 5.2 outlines the finite state machine used to coordinate the half bound behavior of the simulation. The most notable salient feature of the resulting simulation is that the legs sweep much larger angles at the simulation average speed of 3.5 m/s. Notably different from the stiff-back

State	Trigger Event	Actions
LOADING$_A$	Leg A touches down	Zero hip torques on leg A Maintain leg A long length Servo vertebra A straight Position leg B for touchdown Maintain leg B length Servo vertebra B straight
COMPRESSION$_A$	Airspring A reaches positive support	Zero hip torques on leg A Maintain leg A long length **Servo vertebra A down** Position leg B for touchdown Maintain leg B long length Servo vertebra B up
THRUST$_A$	Airspring A reaches maximim compression	Zero hip torques on leg A Thrust with leg A **Servo vertebra A down** Position leg B for touchdown Maintain leg B long length **Servo vertebra B up**
UNLOADING$_A$	Airspring A reaches negative support	Zero hip torques on leg A Shorten leg A **Servo vertebra A down** Position leg B for touchdown Maintain leg B long length **Servo vertebra B up**
FLIGHT$_A$	Leg A leaves ground	Position leg A for touchdown Lengthen leg A Servo vertebra A straight Position leg B for touchdown Maintain leg B length Servo vertebra B straight

Table 5.1: Finite state machine for bounding with vertebral thrust. The state shown in the left column is entered when the event listed in the middle column occurs. The states advance in the listed order continuing on to similar states for the other leg, beginning with COMPRESSION$_B$ and ending with FLIGHT$_B$. All lengths above refer to leg actuator lengths. The items in **boldface** indicate actions which differ from stiff-backed bounding.

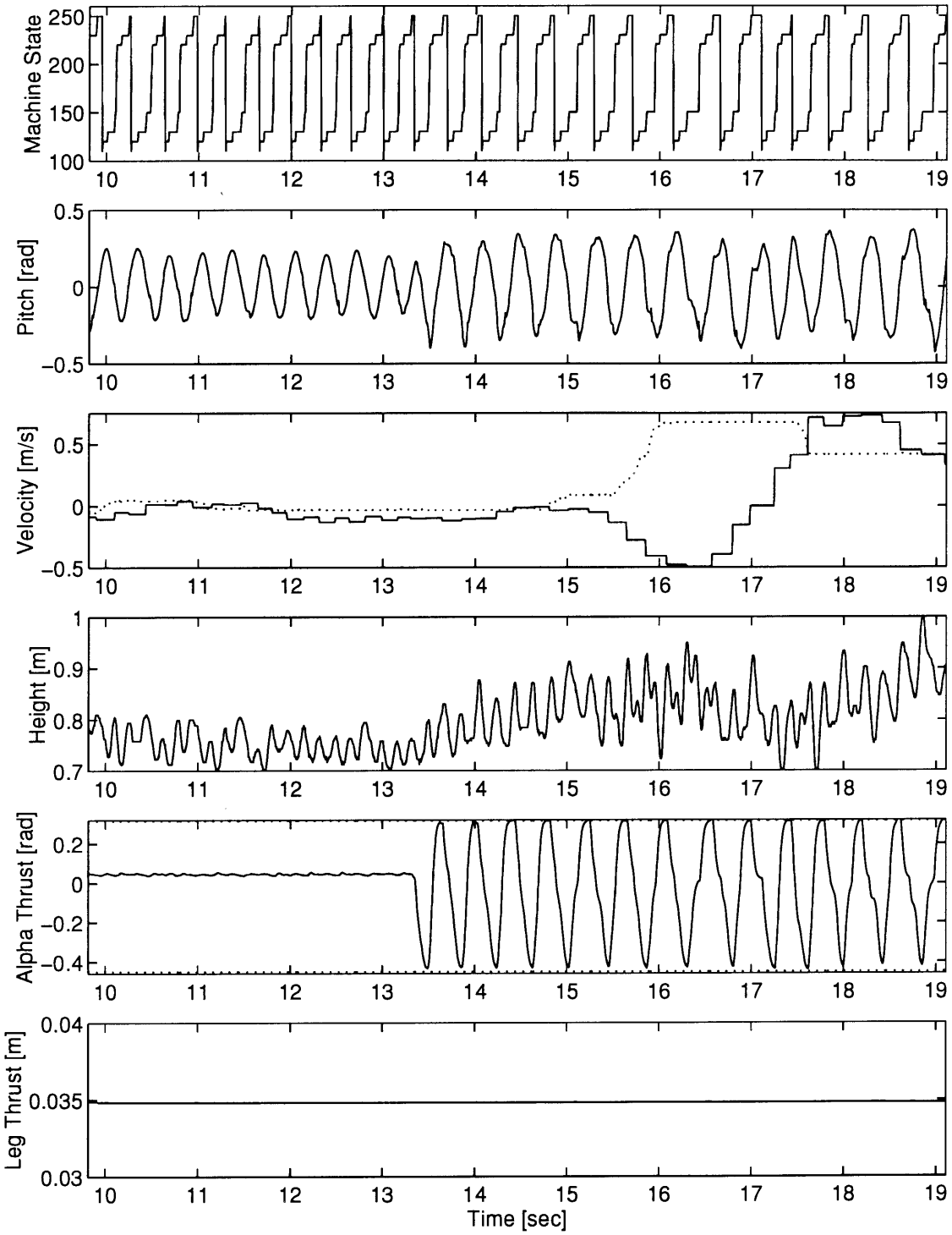

Figure 5-1: Bounding with vertebral thrust data, $\dot{x} \approx 0$ m/s. The dotted line indicates desired values. Solid lines indicate experimental data. Vertebral(α) thrusting begins at approximately $t = 13.3$ seconds. Both hopping height and pitch amplitude increase accordingly.

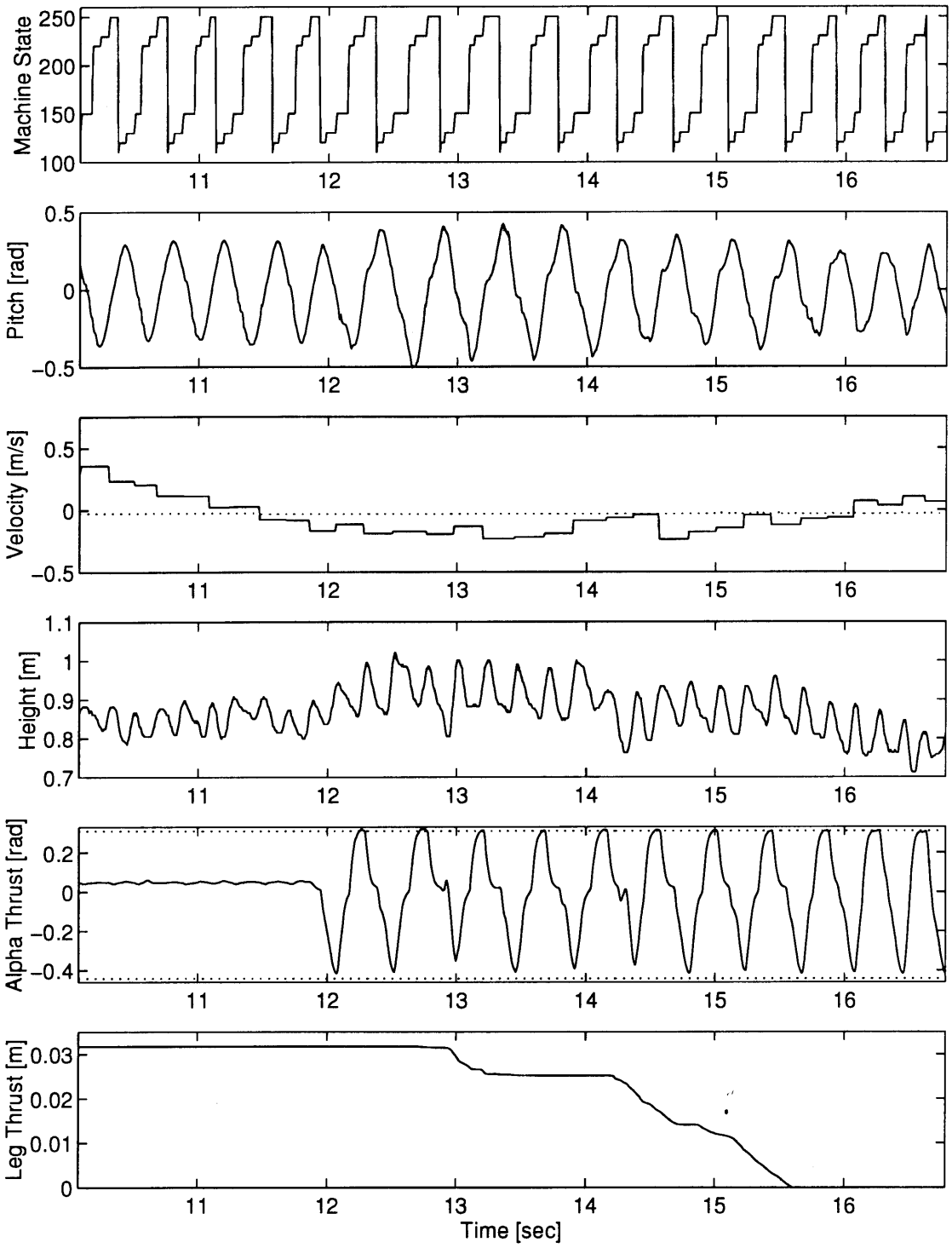

Figure 5-2: Bounding with vertebral thrust data, $\dot{x} \approx 0$ m/s. The dotted line indicates desired values. Solid lines indicate experimental data. Vertebral(α) thrusting begins at approximately $t = 12$ seconds. Both hopping height and pitch amplitude increase accordingly. At about $t = 13$ seconds, leg thrust is slowly decreased until it reaches zero. Hopping height and pitch amplitude decrease below their former values, but the robot maintains the hopping cycle with thrust provided solely by the vertebra.

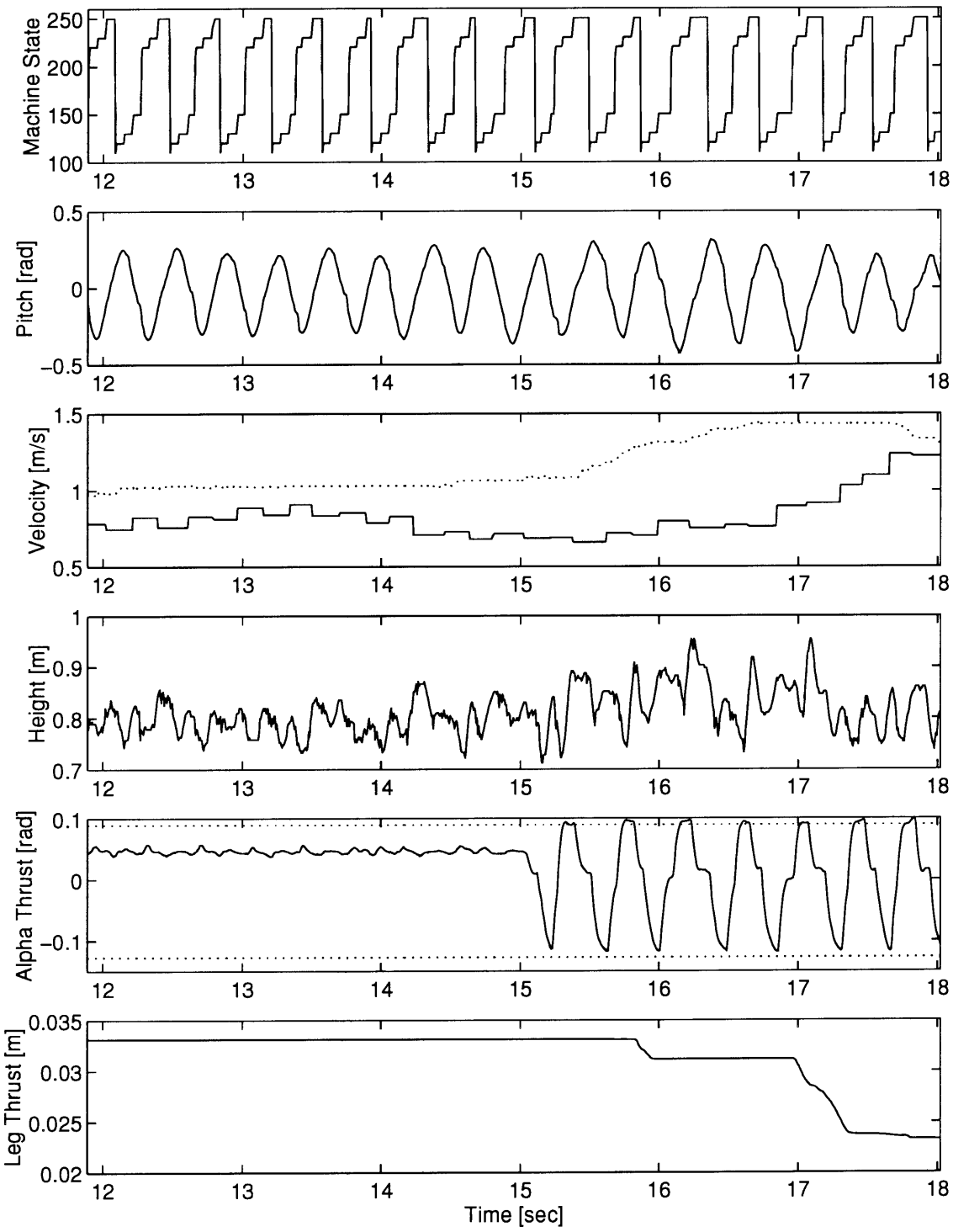

Figure 5-3: Bounding with vertebral thrust data, $\dot{x} \approx .7$ m/s. The dotted line indicates desired values. Solid lines indicate experimental data. Vertebral(α) thrusting begins at approximately $t = 15.0$ seconds. Both hopping height and pitch initially increase accordingly. At about $t = 17.2$ seconds, leg thrust is decreased and hopping height and pitch amplitude return to their former values.

bounding controller is the foot placement law. The feet of the simulation are placed with respect to the approximate center of mass. Specifically, they are placed with respect to the coordinate origin, located where the boom attaches to the robot. The rear leg is always placed at the origin and the foreleg is placed as a function of state:

$$x_{d_f} = \begin{cases} \dot{x}T_s & \text{for fore leg} \\ 0 & \text{for rear leg} \end{cases}$$

where

x_{d_f}	is the planar displacement of the foot from the projection of the center of mass,
T_s	is the duration of the most recent stance period, and
$\dot{x}$	is the average forward speed.

The vertebra angles are commanded to static positions during various states of the locomotion cycle. The desired outcome of this back motion is to decrease the rate that the leg springs would otherwise load, thus increasing ground contact time and the angle swept by the legs during stance. For the fore leg, this action servos the vertebra upwards early in stance. Later, the vertebra is servoed down to maintain force in the leg and allow the mass of the robot to vault over the compressed leg spring. For the rear leg, the vertebra is servoed down during flight to facilitate positioning of the rear leg for touch down. During stance, the vertebra is servoed upwards to decrease loading of the leg spring which would otherwise quickly slow down the robot. This action is coupled with a constant hip torque supplied during the thrust state to help reorient the result ant force vector through the center of mass. However, a joint torque coordination scheme is strictly avoided.

To help prevent the foreleg from stubbing its foot on the ground due to foot placement during FLIGHT_B, the fore leg's hip is servoed to emulate a linear viscous damper,

$$\tau = -B\dot{\theta}$$

where τ is the hip torque, B is a viscous damping coefficient, and $\dot{\theta}$ is the hip rotation rate.

5.3.1 Results

Figure 5-4 depicts the behavior of the simulation over one complete stride under the virtual monopod gait controller. Figure 5-5 displays data from the half bound experiment. The state machine cycles are rather inconsistent and in fact fail several cycles later. Although the velocity and pitch trajectories look consistent, the height trajectories appears possibly period two. Comparison of the vertebra angle (α) graphs shows that there is a marked difference between the fore- and rear vertebra trajectories. The last graph indicates that the feet contact the ground approximately 70% of the state machine cycle time.

Motivation for this experiment came generally from the virtual monopod experiment suggested in Chapter 4. Early attempts at producing similar behavior with the stiff-backed bounding gait seemed to suggest that much softer springs were necessary. That is, without softer springs, the simulation would have short stance durations and for large fore leg excursion angles, the simulation would convert horizontal kinetic energy into vertical kinetic energy, decreasing speed and creating large disturbances to body height. Without resorting to softer springs, I attempted to modify the loading characteristic of the leg spring via motion of the back. The resulting simulation does not produce an actual half bound in the strictest sense, but rather a bound with significant flight time between periods of stance.

Although there is flight time after the fore leg stance period, the duty cycle of ground contact is approximately 70%. This is much greater than the 50% duty cycle experienced by the stiff-backed bounding gait controller. Thus, contact time has increased due to motion of the back.

An interesting result of the simulation is that the programmed behavior for each leg and vertebra pair is not similar. Rather, it is asymmetric. This asymmetry is in contrast to the control

State	Trigger Event	Actions
LOADING$_A$	Leg A touches down	Zero hip torques on leg A
		Maintain leg A long length
		Servo vertebra A up
		Position leg B for touchdown
		Maintain leg B short length
		Servo vertebra B straight
COMPRESSION$_A$	Airspring A reaches positive support	Zero hip torques on leg A
		Maintain leg A long length
		Servo vertebra A up
		Position leg B for touchdown
		Maintain leg B long length
		Servo vertebra B straight
THRUST$_A$	Airspring A reaches maximim compression	**Apply constant hip torque on leg A**
		Thrust with leg A
		Servo vertebra A up
		Position leg B for touchdown
		Maintain leg B long length
		Servo vertebra B up
UNLOADING$_A$	Airspring A reaches negative support	Zero hip torques on leg A
		Shorten leg A
		Servo vertebra A up
		Position leg B for touchdown
		Maintain leg B long length
		Servo vertebra B straight
FLIGHT$_A$	Leg A leaves ground	Position leg A for touchdown
		Maintain leg A short length
		Servo vertebra A straight
		Position leg B for touchdown
		Maintain leg B length
		Servo vertebra B straight

Table 5.2: Finite state machine for half bounding. Leg A is the rear leg. The state shown in the left column is entered when the event listed in the middle column occurs. The states advance in the listed order, proceeding from FLIGHT$_A$ to LOADING$_B$. All lengths above refer to leg actuator lengths. The items in **boldface** indicate actions which differ from stiff-backed bounding.

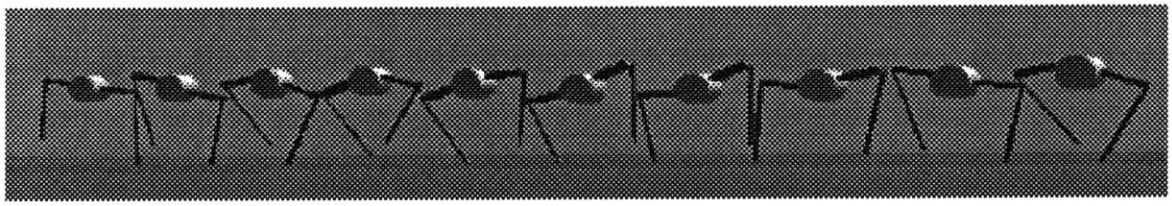

Figure 5-4: Half bound gait. This sequence of frames depicts the behavior of the simulation over one complete stride under the half bound gait controller. In this gait, there are distinct flight phases after each period of ground contact. The data for these frames correspond to that graphed in the right column of Figure 6-7. The frames are temporally spaced .05 seconds apart and separated 1 meter apart.

State	Trigger Event	Actions
LOADING$_B$	Leg B touches down	Zero hip torques on leg B
		Maintain leg B long length
		Servo vertebra B up
		Position leg A for touchdown
		Maintain leg A length
		Servo vertebra A down
COMPRESSION$_B$	Airspring B reaches positive support	Zero hip torques on leg B
		Maintain leg B long length
		Servo vertebra B up
		Position leg A for touchdown
		Maintain leg A long length
		Servo vertebra A down
THRUST$_B$	Airspring B reaches maximim compression	Zero hip torques on leg B
		Thrust with leg B
		Servo vertebra B down
		Position leg A for touchdown
		Maintain leg A long length
		Servo vertebra A up
UNLOADING$_B$	Airspring B reaches negative support	Zero hip torques on leg B
		Shorten leg B
		Servo vertebra B down
		Position leg A for touchdown
		Maintain leg A long length
		Servo vertebra A down
FLIGHT$_B$	Leg B leaves ground	**Servo hip B as a damper**
		Maintain leg B short length
		Servo vertebra B down
		Position leg A for touchdown
		Maintain leg A length
		Servo vertebra A down

Table 5.3: Finite state machine for half bounding, continued. In the above sequence, leg B is assumed the fore leg. The state shown in the left column is entered when the event listed in the middle column occurs. The states advance in the listed order, looping from FLIGHT$_B$ to LOADING$_A$. All lengths above refer to leg actuator lengths. The items in **boldface** indicate actions which differ from stiff-backed bounding.

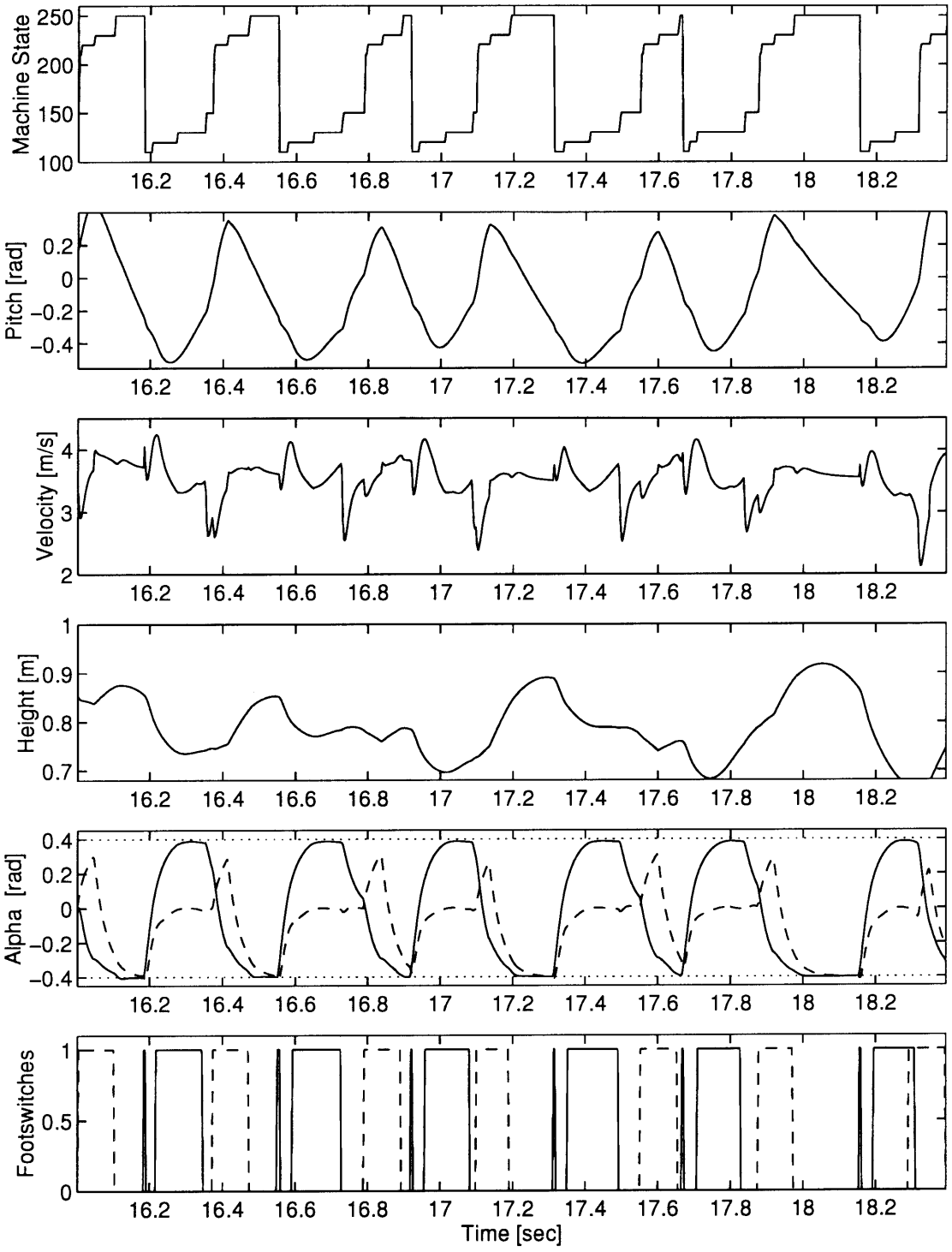

Figure 5-5: Half bounding data. The dotted line indicates desired values. Solid lines indicate experimental data. Dashed lines represent the fore leg, leg B. Solid lines indicate experimental body or leg A data. A nonzero value for a footswitch means the foot is in contact with the ground. As labeled in Appendix A, α_A and α_B correnspponds to the rear and fore legs respectively.

approach of previous leg lab robots where control for each leg was identical. The necessity of such a phenomenon may be an artifact that half bounding in a manner such as presented herein is a steady state behavior that only becomes apparent far from zero velocity. This fact brings up an interesting point. The behavior of the simulation is more analogous to a gallop and there exists a speed below which an animal does not normally gallop. This trot-gallop transition speed is predicted as 3.3 m/s for a 25 kg animal [20]. Animals have been trained to gallop slightly below their normal trot-gallop transition speed [18]. Maybe gaits such as a bound are undefined for very low velocities since the legs cannot experience significant excursions when the speeds are small.

The method of foot placement in the half bounding simulation is appealing. For stiff-backed bounding, the feet were placed with respect to the hips. However, it is the trajectory of the center of mass that I wish to control. In the half bound simulation, over a stride, the legs sweep roughly symmetric angles. To do this, though, one leg sweeps roughly ahead of the center of mass and one sweeps behind. Thus, a long stride is obtained using leg sweeps that individually do not have an axis of symmetry, yet the motions of the two legs are roughly symmetric to each other.

5.4 Impedance Servo

Section 4.2 discussed the strategy of treating the Planar Quadruped as a virtual monopod. To the extent that the half bound controller allowed the workspaces of the fore and rear leg to slightly overlap, it resembled the virtual monopod control approach. Unsatisfied and compelled with the virtual monopod control strategy, I modified the half bound gait controller to eliminate the second flight phase and more closely emulate a virtual monopod. Such a strategy required landing on the fore leg, transfering support below the center of mass in a brief double support phase, and taking off from rear leg. By transferring support under the body, the full workspace of both legs was used, preserving monopod-like symmetry.

Section 5.3 described a gait controller that was stable for at least six strides even though control of the vertebra behavior was not related to any system parameters or state. In that sense, control was open loop. It seemed plausible then that if the vertebra can be used in open loop fashion to modify the leg spring impedance characteristic, then maybe this could happen with improved performance in closed loop form. To test my hypothesis, I needed a performance metric related to the leg impedance and one that that vertebra motion could strongly influence. Ideally, the monopod would experience a single bounce per virtual stance period. Thus, I reasoned that both legs should be used sequentially to impart a vertical force on the center of mass to give rise to this motion. The vertical ground reaction force appeared to be the appropriate performance metric. However, it was difficult to believe that a static force trajectory would be stable. As such, I chose to introduce the dynamics of a virtual vertical Hookean spring. The causality is well-matched to the process at hand–the robot's mass moves; that motion causes a deflection in the spring which generates a force; the mass moves in response to the applied force. In addition, as demonstrated in Section 5.1, vertebra motion can influence the vertical dynamics. The new gait controller servoed the vertebra according to the simple proportional law:

$$\tau_v = K_f(F_{d_z} - F_z),$$

where

τ_v	is the vertebra torque,
F_{d_z}	is the desired vertical reaction force,
F_z	is the vertical ground reaction force, and
K_f	is a gain.

The desired vertical reaction is defined as

$$F_{d_z} = K(z_{td} - z),$$

where

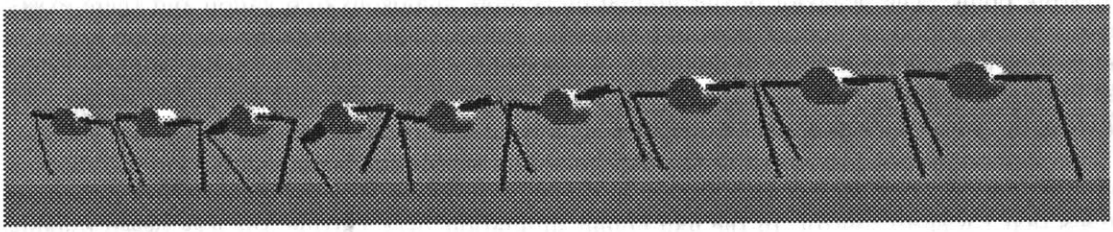

Figure 5-6: Virtual monopod gait. This sequence of frames depicts the behavior of the simulation over one complete stride under the virtual monopod gait controller. Note that in the third frame both feet are in contact with the ground and that a only single aerial phase exists, occurring after the hind foot leaves the ground. The data for these frames correspond to that graphed in the left column of Figure 6-7. The frames are temporally spaced .05 seconds apart and separated 1.1 meter apart.

z_{td}	is the vertical height of the robot at touchdown,
z	is the vertical height of the robot, and
K	is a virtual vertical spring constant, $K = 7000$ N/m.

5.4.1 Results

Figure 5-6 depicts the behavior of the simulation over one complete stride under the virtual monopod gait controller. Figure 5-7 displays data from this experiment. Although, the gait was not stable for more than a couple of cycles, the simple control law resulted in acceptable tracking of F_{d_z}. Spikes in the ground reaction force plot are due to force transients at touchdown due to the ground contact model dynamics and from individual leg thrusts which generated a disturbance that the impedance servo attempted to reject. As expected, the footswitch data overlaps, indicating a period of double support as desired by the gait controller.

The primary result of this experiment can be seen by comparison of the vertebra trajectories for the half bound and for the impedance servo experiments. For both experiments, the vertebra angle trajectories are similar. In the half bound experiment, the vertebra angles were specifically commanded to various static positions during various parts of the locomotion cycle, so the vertebra angle trajectory is a direct consequence of this explicit programming. However, in the impedance servo experiment, the trajectory is a result of interaction of the robot dynamics and the simulated vertical spring. The similarities might suggest that such an impedance servo and gait controller could lead to a gait that is at least as stable as that produced by the half bound controller.

Although a small amount of individual leg thrust was used in this experiment, an intriguing strategy might be to eliminate leg thrust altogether in the fore leg and coordinate behavior in the rear leg to produce a thrust force. This thrust force could be applied when the virtual vertical spring reached maximum compression, just as leg thrust is applied when an airspring becomes fully compressed. Such a controller would be appealing because it would fit nicely into the framework of using a controller for a simple machine, in this case a monopod, and imposing dynamic constraints such that a more complex machine behaves as the simpler one. This strategy has been shown to be effective for the control of other Leg Lab robots [24] [25].

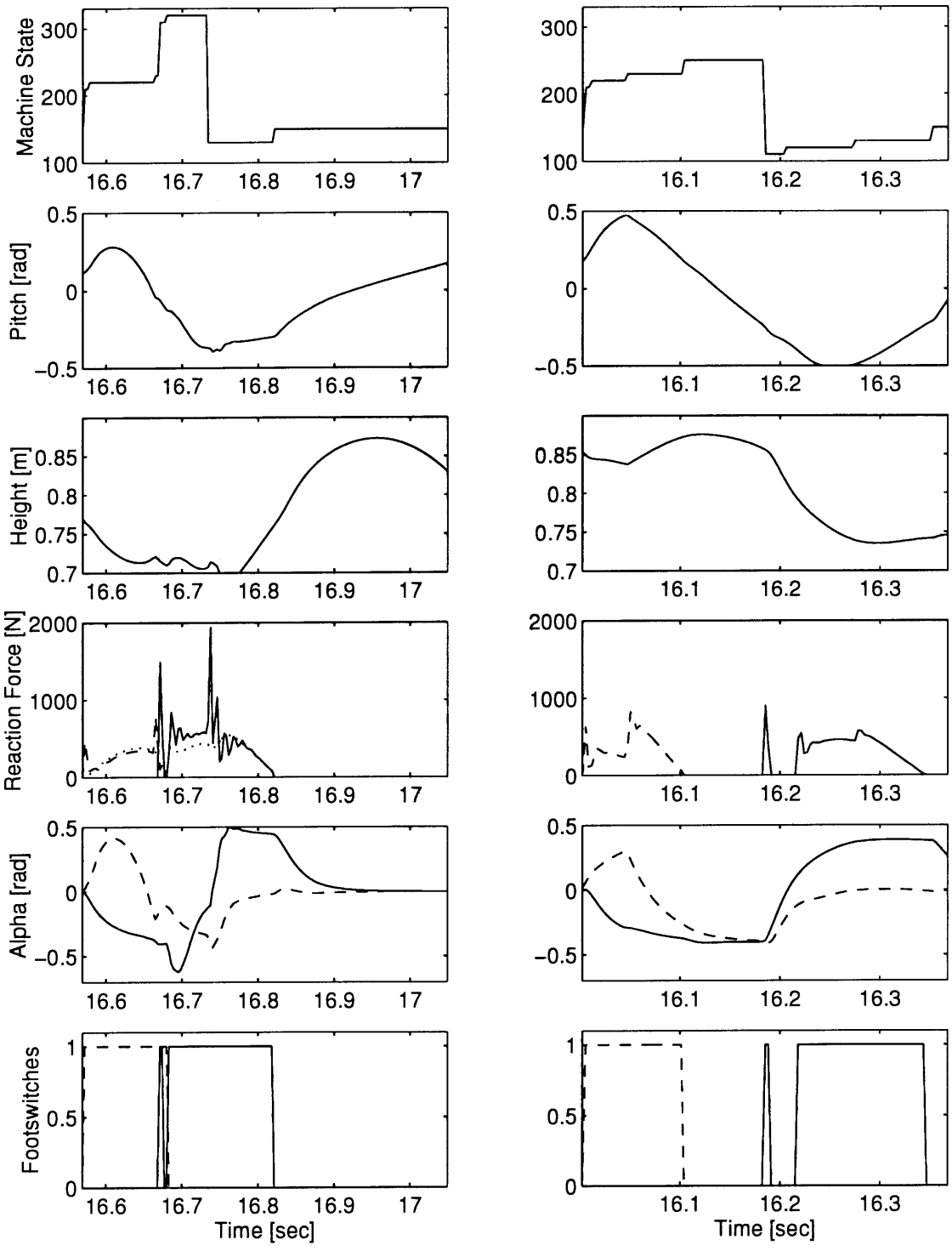

Figure 5-7: Comparison of impedance servo data(left) and half bounding data (right) for one complete cycle of the state machine. Dotted lines are desired vertical force values. Dashed lines represent the fore leg, leg B. Solid lines indicate experimental body or leg A data. A nonzero value for a footswitch means the foot is in contact with the ground. As indicated by comparison of the profiles of the vertebra(α) angles, servoing the vertebra off a desired impedance characteristic produces vertebra angle trajectories similar to those generated by commanding the vertebra to static positions.

Chapter 6

Conclusion

Mammalian quadrupeds perform amazing feats of endurance and speed. Inspired by their remarkable ability, in this thesis, I explored the role of a spine in quadruped running. I reviewed the biomechanical literature and discussed possible experiments to explore some of the conventional and unconventional benefits of a quadruped spine.

I described a planar robot used as a test platform for experiments and evaluation of control strategies. The hydraulic machine has two telescoping, springy legs with actuated hips, one fore and one aft. Although the Planar Quadruped only has two legs, the arrangement simplifies the design yet captures the dominant leg behavior found in bounding. Spanning the hips is an articulated spine composed of three segments with actuated joints.

Experiments with the Planar Quadruped robot reveal that thrusting with the back can be used to augment the thrust provided by the legs. I performed an experiment that exploits the series kinematic connection between the back and the foot. In the experiment, motion of the back was used to modulate the energy state of the leg spring.

Simulation experiments suggest that motion of the back can be used to modify the impedance characteristic of the legs. I performed two experiments to explore this possibility. The first commanded the joints of the back to open loop static positions during various parts of the locomotion cycle to reduce the rate of compression of the leg springs. The second attempted to servo these joints off of the ground vertical reaction force to simulate a virtual vertical spring. Although only partially successful, the second appears very promising. In the process, I developed two interesting gait controllers that coordinates the behavior of the robot to produce a bounding gait with significantly larger leg workspaces than a previous Leg Lab quadruped robot [11] [24].

Chapter 7

Future Work

7.1 Energy Storage and Transfer

Section 2.3 introduced the possibility that the spine may play a significant energy storage and transfer role during quadrupedal running. Later, in Section 4.6, I presented possible areas of study that could lead to experiments exploring this phenomenon. In this section, I would like to suggest a radically different model for the spine and its effect on running locomotion.

The model for the spine that I propose is unlike the general design of the Planar Quadruped robot. Rather, it derives from the mass-spring-mass model shown in Figure 7-1. The system consists of a translational mass connected to another translational mass by a single degree of freedom linear spring. Such a system has two passive vibratory modes. One is the zero frequency mode where both masses translate with the same velocity with no deflection in the spring. The second mode is antagonistic and the mass velocities are opposite in sign. As a linear system, the modes superpose and the system can travel with an inchworm-like appearance.

This inchworm effect is not unlike some of the behavior observed in the spine of a running cheetah. When the rear legs are on the ground, the spine is observed to extend, accelerating the forequarters. Similarly, while the forelegs are on the ground, the rear legs are pulled towards the forequarters. At 45 mph, this motion causes the forelegs to travel 3.5 feet per second faster than the center of mass [14].

Figure 7-2 shows how this model might be applied to the design of another robot or simulation to study back motion. The articulated spine is replaced with a single linear spring in parallel with a force actuator. The trunk still has significant mass, but with this kinematic arrangement, the masses in the body cannot rotate with respect to one another. This quadruped design is conceptually similar to the middle system model described in Figure 4-4. In that model, causality suggested that a single spring could satisfactorily connect the front and rear leg hoppers. A force source in parallel with the spring also satisfies causality. This force source might be used to servo an impedance as suggested in Section 4.6 where a system with a nominal vibratory frequency could be forced to vibrate at a different frequency if the actuator provide an apparent change in back stiffness.

This linear spine model might prove useful for additional study of back motion. Although its frequency of spinal vibration is in reality very complex due to interaction with the ground via the legs, it might be possible to make those effects less significant by making the body mass large compared to the leg mass. It is also true that the behavior of a real animal spine is very complex. Is it reasonable to even consider such a simple linear spring model for the spine? Animal legs are also complex organs whose dynamic behavior has been successfully simplified to a single linear stiffness that acts along the leg [21]. This model has been found to be applicable over a wide range of speeds[9]. It would be interesting to discover that such a simple model might apply to the spine as well.

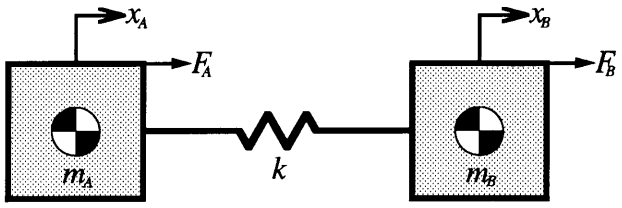

Figure 7-1: Mass-spring-mass system. The system consists of a translational mass connected to another translational mass by a single degree of freedom linear spring. Such a system has two passive vibratory modes that can superpose, resulting in an inchworm-like motion.

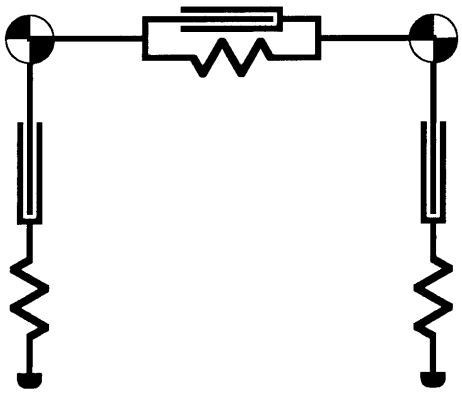

Figure 7-2: Linear spine model. The articulated spine of the Planar Quadruped model is replaced with a single linear spring in parallel with a force actuator. The trunk still has significant mass, but with this kinematic arrangement, the masses in the body cannot rotate with respect to one another.

7.2 Control of Flight Time

Section 4.3 mentioned how control of the body inertia could be used to maximize flight time in order to optimize the distance travelled during flight, maximizing stride length. Concerns such as this become increasingly important as the robot travels faster. In this section, I describe some of the relationship between flight time and the rigid body rotational dynamics of a quadruped robot. Afterwards, I present a means of servoing the rotational take off state via a coordinated actuation scheme during stance.

Hopping is a resonant oscillation of the body mass on springy legs in a gravitational field. For all of the Leg Lab hopping robots, elastic potential energy during stance is converted to kinetic energy which later is converted to gravitational potential energy. For bipedal robots, this oscillation involves energy storage in the form of vertical linear momentum. Unlike the bipedal robots, the angular and vertical linear dynamics are highly coupled for a bounding quadruped due to the displacement of the hips from the center of mass. As such, the bounce frequency is not only a function of the vertical leg length and the trajectory of the center of mass, but of the angular trajectory as well. If the bounce frequency can be reduced by increasing the flight time, the control effort required of the actuators diminishes and stride length increases.

Referring to Figure 7-3 diagramming take off from the rear leg A and rotating in the negative ϕ direction, the height trajectory of the descending foot B is

$$z_f(t) = z_{com}(t) + r\sin(\phi(t)) - l_z \tag{7.1}$$

where z_f is the vertical height of the foot, z_{com} is the height of the center of mass, r is the displacement of the hip from the center of mass, and l_z is the vertical leg length. The trajectory of the center of mass is

$$z_{com} = \frac{1}{2}gt^2 + \dot{z}_0 t + z_0, \tag{7.2}$$

where g is the acceleration of gravity and $_0$ subscripts denote take off conditions. For simplicity, if we for now assume that the inertia of the body is constant, $\frac{d}{dt}J_f = 0$, then

$$\phi = \dot{\phi}t + \phi_0. \tag{7.3}$$

Combining equations results in the following:

$$z_f(t) = 0 = \frac{1}{2}gt^2 + \dot{z}_{b0}t + z_{b0} + r\sin(\dot{\phi}_0 t + \phi_0) - l_z. \tag{7.4}$$

For small ϕ:

$$0 = \frac{1}{2}gt^2 + \dot{z}_{b0}t + z_{b0} + r(\dot{\phi}_0 t + \phi_0) - l_z$$

yielding the quadratic equation

$$0 = \frac{1}{2}gt^2 + (\dot{z}_{b0} + r\dot{\phi}_0)t + (z_{b0} + r\phi_0 - l_z).$$

Using the quadratic formula,

$$t_f = \left\{ - \left[\frac{\dot{z}_{b0} + r\dot{\phi}_0 \pm \sqrt{\dot{z}_{b0}^2 + 2\dot{z}_{b0}r\dot{\phi}_0 + r^2\dot{\phi}_0^2 - 2g\dot{z}_{b0} - 2gr\phi_0 + 2gl_z}}{g} \right] \right\} \tag{7.5}$$

The solution corresponding to the plus sign next to the radical is the positive, real solution. To be thorough, the flight time is really the minimum of the time it takes the fore and rear legs to touchdown:

$$t_f = \min\left\{t_{f_{front}}, t_{f_{rear}}\right\}.$$

One could imagine a case where the robot just hopped on its rear leg. In order that the robot

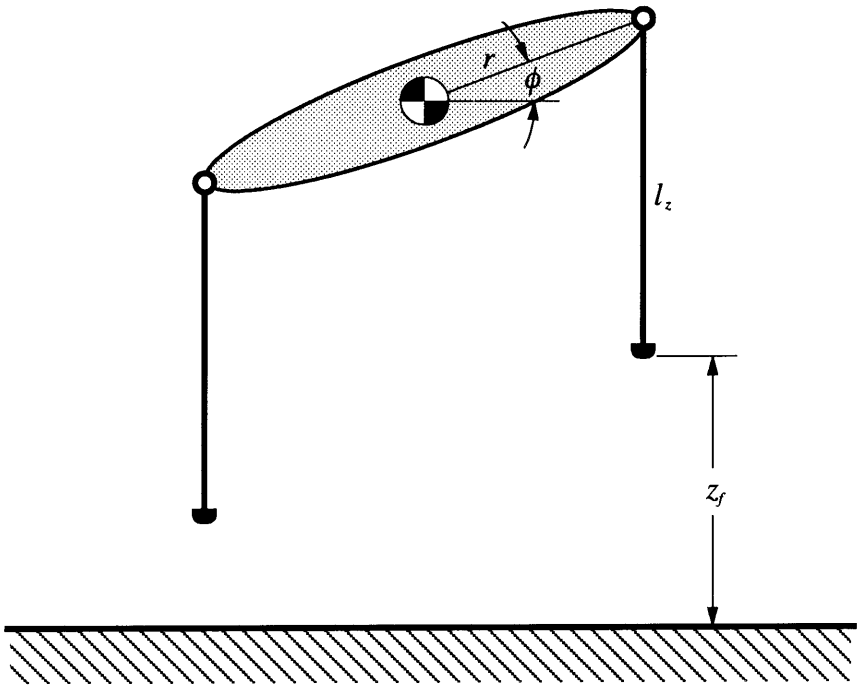

Figure 7-3: Height of the descending foot. Here, a quadruped robot has just gone into flight from the rear leg A, rotating in the negative ϕ direction. Touchdown will occur when foot B strikes the ground, unless foot A strikes first.

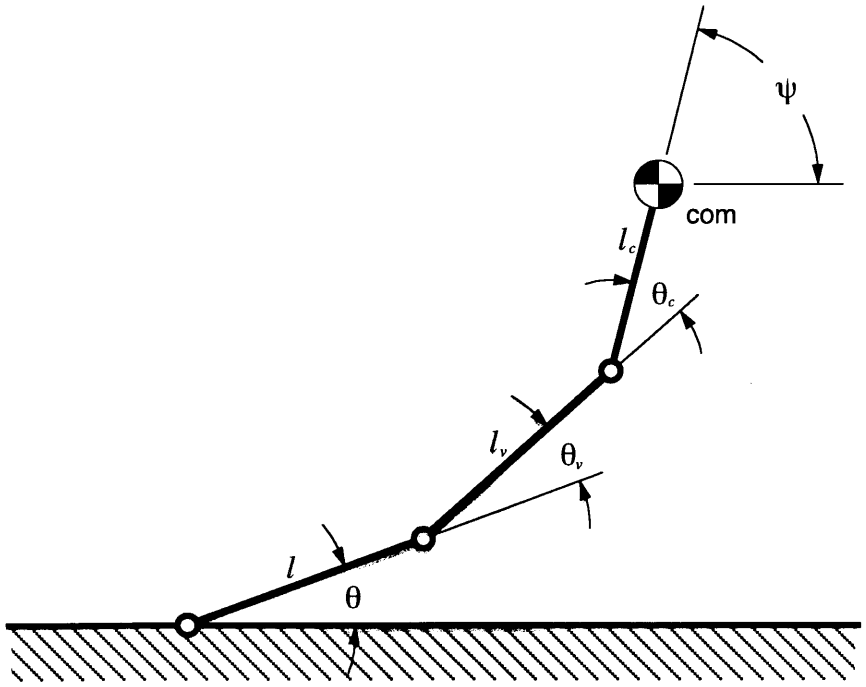

Figure 7-4: Kinematic diagram for deriving a tensor relationship between joint torques and applied forces and torques on the body's center of mass. The center of mass is assumed to lie in the center of the cage segment. Half the cage length is l_c. The length of the vertebra segment is denoted l_v.

lands on its front leg after leaving the ground on its rear leg, we can subject the solutions to the constraint that

$$\phi_{td} = \dot{\phi}_0 t_f + \phi_0 \leq 0.$$

For symmetric touchdown conditions, t_f is maximum for

$$\phi_0 = -\phi_{td} = 0$$

$$\dot{\phi}_0 = \dot{\phi}_{td} = 0.$$

That is, flight time for a quadruped with a rigid body is maximized when the overall bouncing behavior resembles a biped with no significant rotational dynamics. However, the Planar Quadruped has the ability to reconfigure its body during flight. As such, the optimal angular rigid body trajectory might differ from the conditions given above. Determination of such an optimal trajectory is recommended for future work.

Once a trajectory for the center of mass is determined, it is possible to construct a coordinated servo to drive the system to the proper take off conditions. A relationship between actuator joint forces and torques and applied forces and torques on the body's center of mass is found by determining a Jacobian matrix for the serial chain connecting the ground to the center of mass as diagrammed in Figure 7-4. The center of mass is assumed to lie in the center of the cage segment. Half the cage length is l_c. The length of the vertebra segment is denoted l_v. The angle notation in Figure 7-4 is related to Planar Quadruped parameters as

$$\theta_v = -\beta$$

$$\theta_c = -\alpha$$

$$\psi = \phi + \pi$$

$$\theta = \phi + \pi + \alpha + \beta.$$

Starting at the ground and working out towards the center of mass, time differentiation of the forward kinematic map results in the manipulator Jacobian matrix. A tensor relationship exists relating actuator forces to forces at the end of the kinematic chain, in this case the center of mass:

$$\begin{bmatrix} \tau_\theta \\ \tau_\beta \\ \tau_\alpha \\ F_l \end{bmatrix} = \mathbf{J}^T \begin{bmatrix} F_x \\ F_z \\ \tau_\phi \end{bmatrix} = \begin{bmatrix} j11 & j21 & 1 \\ j12 & j22 & -1 \\ j13 & j23 & -1 \\ j14 & j24 & 0 \end{bmatrix} \begin{bmatrix} F_x \\ F_z \\ \tau_\phi \end{bmatrix}, \tag{7.6}$$

where the entries of this Jacobian matrix are as defined in Section A.3. This system of four equations is subject to two constraints. One, no torque can be applied between the foot and the ground due to point contact:

$$\tau_\theta = 0.$$

Two, the force in the leg spring is determined by the body dynamics and cannot be servoed. However, it can be measured:

$$F_l \equiv \text{measured}.$$

Thus, there is one free variable that we can specify. We choose the torque on the body:

$$\tau_\phi \equiv \text{specified}.$$

Addition of these three constraints yields seven equations in seven unknowns.

During stance, the body can be compelled toward a desired angular state trajectory via a torque defined as

$$\tau_\phi = K_\phi(\phi_d - \phi) + K_{\dot\phi}(\dot\phi_d - \dot\phi). \tag{7.7}$$

The system of equations can be solved for the necessary joint torques that satisfy the above constraints:

$$\begin{bmatrix} \tau_\beta \\ \tau_\alpha \\ F_x \\ F_z \\ \tau_\theta \end{bmatrix} = \frac{1}{j21j14 - j24j11} \begin{bmatrix} j24j11 + j24j12 - j21j14 - j22j14 & j12j21 - j11j22 \\ j24j11 + j24j13 - j21j14 - j23j14 & j13j21 - j11j23 \\ j24 & j21 \\ j14 & j11 \\ 0 & 0 \end{bmatrix} \begin{bmatrix} \tau_\phi \\ F_l \end{bmatrix} \tag{7.8}$$

The above scheme can be used to apply torques about the center of mass. Gait control strategy could then be:

- Control hopping height as before with leg thrust since the leg spring remains the dominant vertical effect
- Control forward running velocity via foot placement
- Control pitching frequency and therefore maximize flight time by use of (7.7).

Since it is not possible to exert torques about the foot ($\tau_\theta = 0$), the space of the solution is only two dimensional. Thus, although we may be able to supply an arbitrary static torque, τ_ϕ about the center of mass, the resultant forces, F_x and F_z, cannot be specified. As such, undesireable coupling between attitude correction and vertical motions may result, but this is not traumatic since such coupling can be treated as disturbances to other parts of the gait controller.

The coordinated strategy described above is based on a static relationship between actuator and center of mass forces and torques. However, during dynamic running, inertial forces can be large. Nevertheless, the servo law incorporates some robustness which is a function of choice of gains. Thus, performance may be satisfactory under dynamic conditions even though the derivation is static.

Appendix A

Kinematics

A.1 Robot Coordinates

Joint angles are defined positive counter clockwise per standard convention on the right leg in Figure A-1. They are define positive clockwise for the left leg to allow the same kinematic transformations to be used for both legs with only a minor sign change in pitch.

A.2 Joint-Actuator Space Transformation

As shown in Figure A-2, the actuator space kinematics are similar by design for both the hip and vertebra joints. The forward kinematic map from actuator to joint space is simply:

$$c_i = \cos^{-1}\left(\frac{l_1^2 + l_2^2 - w_i^2}{2l_1 l_2}\right)$$

$$\beta = -c_\beta$$

$$\alpha = c_\alpha - \pi/2$$

where i denotes the angle subscript, either α or β. The inverse kinematic map from joint to actuator space is:

$$c_\beta = -\beta$$

$$c_\alpha = \alpha + \pi/2$$

$$w_i = \sqrt{l_1^2 + l_2^2 - 2l_1 l_2 \cos(c_i)}.$$

The actuator moment arm is computed as

$$r_i = \frac{l_1 l_2 \sin(c_i)}{w_i}.$$

Other standard transformations, such as joint to cartesian space, are omitted for brevity.

A.3 Foot-to-COM Jacobian Matrix

Joint velocities of the stance leg are related to the cartesian velocity of the center of mass by the manipulator Jacobian matrix:

b

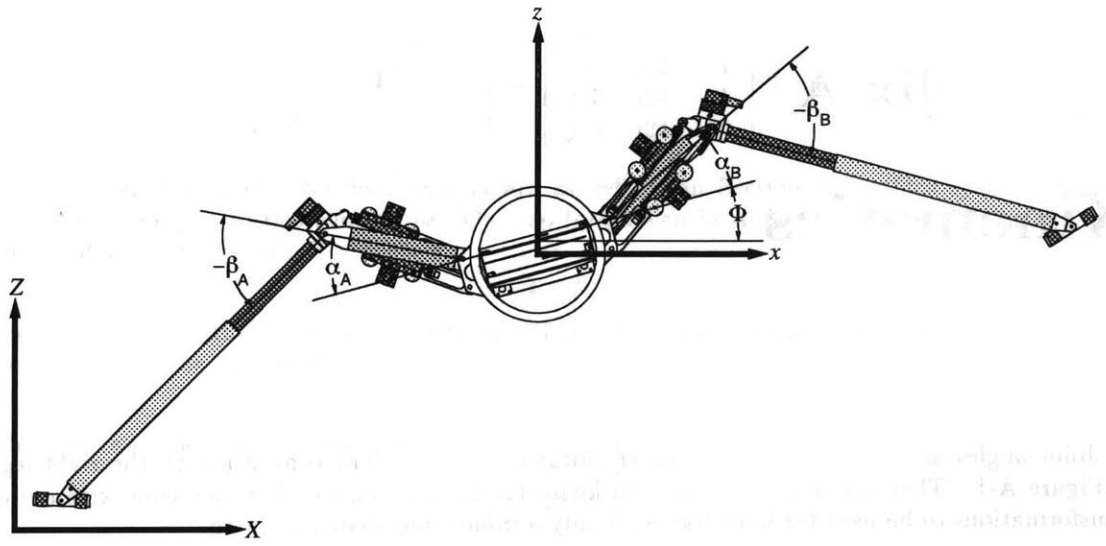

Figure A-1: Assignment of robot coordinate frames and definition of positive angles. ϕ is the robot's absolute pitch. α is the relative angle of the vertebra joint. β is the relative angle of the hip joint.

$$\begin{bmatrix} \dot{x} \\ \dot{z} \\ \dot{\psi} \end{bmatrix} = \mathbf{J} \begin{bmatrix} \dot{\theta} \\ \dot{\beta} \\ \dot{\alpha} \\ \dot{l} \end{bmatrix} = \begin{bmatrix} j11 & j12 & j13 & j14 \\ j11 & j12 & j13 & j14 \\ 1 & -1 & -1 & 0 \end{bmatrix} \begin{bmatrix} \dot{\theta} \\ \dot{\beta} \\ \dot{\alpha} \\ \dot{l} \end{bmatrix}.$$

The matrix entries are as follows:

$$j11 = -l\sin(\theta) - l_c\sin(\theta-\beta) - l_v\sin(\theta-\beta-\alpha)$$

$$j12 = l_c\sin(\theta-\beta) + l_v\sin(\theta-\beta-\alpha)$$

$$j13 = l_v\sin(\theta-\beta-\alpha)$$

$$j14 = \cos(\theta)$$

$$j21 = l\cos(\theta) + l_c\cos(\theta-\beta) + l_v\cos(\theta-\beta-\alpha)$$

$$j22 = -l_c\cos(\theta-\beta) - l_v\cos(\theta-\beta-\alpha)$$

$$j23 = -l_v\cos(\theta-\beta-\alpha)$$

$$j24 = \sin(\theta).$$

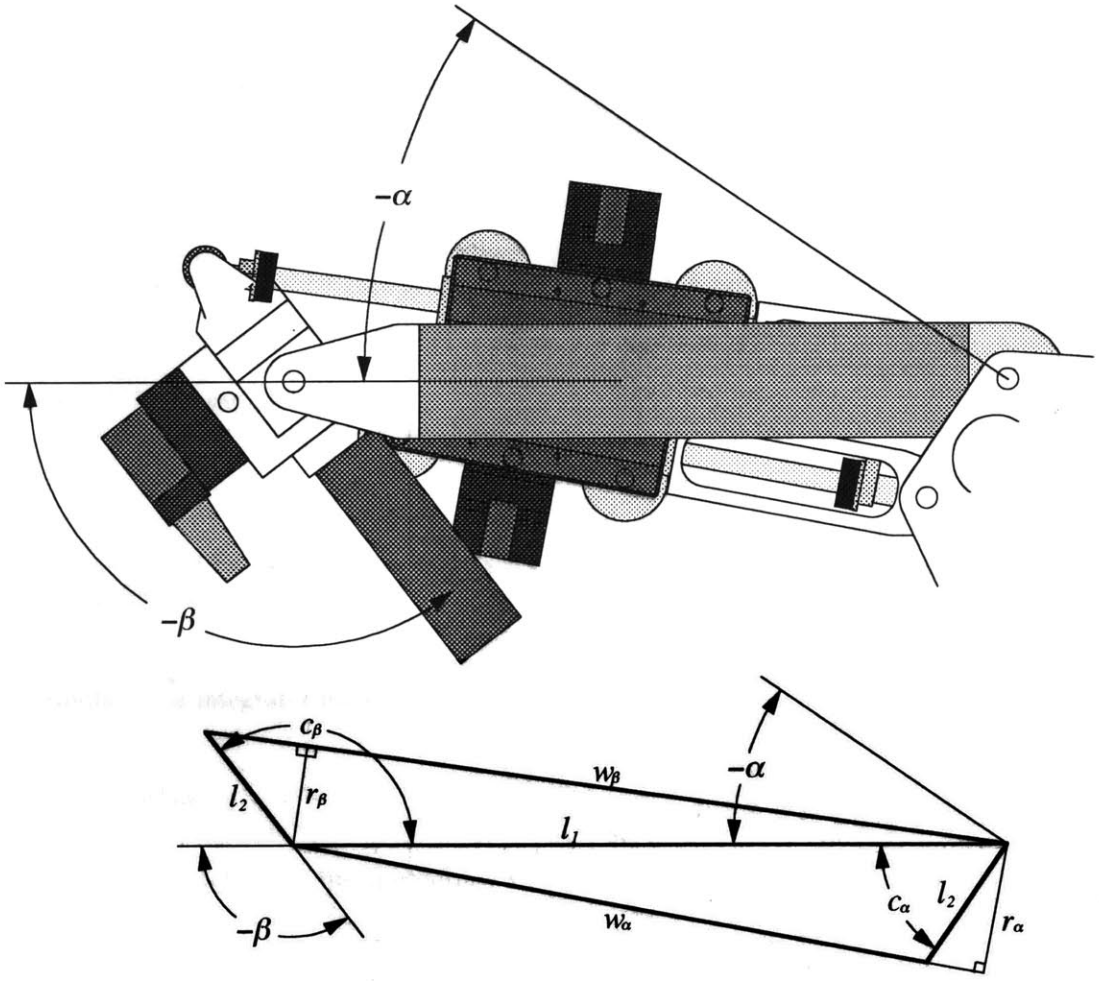

Figure A-2: Actuator kinematics. Angles α and β correspond to angles defined in Figure A-1. The actuator space kinematics are similar by design for both the hip and vertebra joints.

Appendix B

Filters

Signal differentiation was approximated discretely via forward emulation of a continuous derivative passed through a first order lag with pole at a,

$$y(s) = \frac{as}{s+a}x(s)$$

where $a < 2\pi f_{Nyq}$. For the leg boards where the filters operated, $f_{Nyq} = 252$ Hz. Using the zero order hold method of discretization, the following difference equation results:

$$y_t = (1 - aT)y_{t-1} + a(x_t - x_{t-1}),$$

where $1/T$ is the sample rate.

A low pass filter of the continuous form

$$y(s) = \frac{a}{s+a}x(s)$$

was implemented by applying the backward difference method of discretization, resulting in the following difference equation:

$$y_t = \frac{aTx_t + y_{t-1}}{1+aT}.$$

Similarly, an integrator filter

$$y(s) = \frac{1}{s}x(s)$$

was implented as

$$y_t = Tx_t + y_{t-1},$$

where y_0 was initialized to the appropriate value.

Bibliography

[1] R. M. Alexander. *The Chordates.* Cambridge University Press, Cambridge, 1975.

[2] R. M. Alexander. Elastic energy stores in running vertebrates. *American Zoology*, 24:85–94, 1984.

[3] R. M. Alexander. Why mammals gallop. *American Zoology*, 28:237–245, 1988.

[4] R. M. Alexander. Three uses for springs in legged locomotion. *The International Journal of Robotics Research*, 9(2):53–61, 1990.

[5] R. M. Alexander, N. J. Dimery, and R. F. Ker. Elastic structures in the back and their role in galloping in some mammals. *Journal of Zoology, London*, 207:467–482, 1985.

[6] R. M. Alexander and A. S. Jayes. Estimates of the bending moments exerted by the lumbar and abdominal muscles of some animals. *Journal of Zoology, London*, 194:291–303, 1981.

[7] G. A. Cavagna, N. C. Heglund, and C. R. Taylor. Mechanical work in terrestrial locomotion: Two basic mechanisms for minimizing energy expenditure. *American Journal of Physiology*, 233:243–261, 1977.

[8] R. B. Chiasson. *Laboratory Anatomy of the Cat.* Wm. C. Brown, Dubuque, Iowa, 1989.

[9] C. T. Farley, J. Glasheen, and T. A. McMahon. Running springs: speed and animal size. *Journal of Experimental Biology*, 185:71–86, 1993.

[10] M. A. Fedak, N. C. Heglund, and C. R. Taylor. Energetics and mechanics of terrestrial locomotion ii. kinetic energy changes of the limbs and body as a function of speed and body size in birds and mammals. *Journal of Experimental Biology*, 79:23–40, 1982.

[11] J. Furusho and A. Sano. Quadruped. In *Dynamic Walking by Legged Locomotion Robots*, Japan, 1984–1990. Gifu University. Video tape.

[12] P. P. Gambaryan. *How Mammals Run.* Keter Press Publishing House, Jerusalem, 1974.

[13] J. Gray. *How Animals Move.* Cambridge University Press, London, 1960.

[14] M. Hildebrand. Motions of the running cheetah and horse. *Journal of Mammology*, 40(4):481–495, 1959.

[15] M. Hildebrand. How animals run. *Scientific American*, pages 148–157, 1960.

[16] A.V. Hill. The heat of shortening and the dynamic constants of muscle. *Proceedings of the the British Royal Society*, 126:136–195, 1938.

[17] S. Hirose. A study of design and control of a quadruped walking vehicle. *International J. Robotics Research*, 3:113–133, 1984.

[18] D. F. Hoyt and C. R. Taylor. Gait and the energetics of locomotion in horses. *Nature*, 292:239–240, 1981.

[19] J. Koechling and M. Raibert. How fast can a legged robot run? In *Symposium in Robotics DSC-Vol.1*, New York, 1988. American Society of Mechanical Engineers. K. Youcef-Toumi and H.Kazerooni (eds.).

[20] T. A. McMahon. *Muscles, Reflexes, and Locomotion.* Princeton University Press, Princeton, 1984.

[21] T. A. McMahon. The role of compliance in mammalian running gaits. *Journal of Experimental Biology*, 115:263–282, 1985.

[22] H. Miura, I. Shimoyama, M. Mitsuishi, and H. Kimura. Dynamical walk of quadruped robot (collie-1). In *Second International Symposium on Robotics Research*, pages 317–324, Cambridge, 1985. MIT Press. H. Hanafusa and H. Inoue (eds.).

[23] E. Muybridge. *Muybridge's Complete Human and Animal Locomotion, vol. III.* Dover Publications, Inc., New York, 1979.

[24] M. H. Raibert. Four-legged running with one-legged algorithms. In *Second International Symposium on Robotics Research*, pages 311–315, Cambridge, 1985. MIT Press. H. Hanafusa and H. Inoue (eds.).

[25] M. H. Raibert, M. Chepponis, and H. B. Brown Jr. Running on four legs as though they were one. *IEEE J. Robotics and Automation*, 2, 1986.

[26] Marc H. Raibert. *Legged Robots that Balance.* MIT Press, Cambridge, MA, 1986.

[27] Marc H. Raibert. Quadruped trotting, pacing, and bounding. *Dynamically Stable Legged Locomotion, Final Report: September 1985–August 1988*, pages 115–139, 1989. Artifical Intelligence Laboratory, MIT.

[28] Marc H. Raibert. Trotting, pacing and bounding by a quadruped robot. *Journal of Biomechanics*, 23, 1990.

[29] Robert Ringrose. The creature library. Unpublished reference guide to a C library used to create physically realistic simulations, 1992.

[30] K. Yamafuji. The robot cat. In *The Robot Cat and Another Robot of Yamafuji Lab*, Japan, 1992. Yamafuji Lab, University of Electro-Communications. Video tape.

467-16